

**MODELING AND RHEOLOGY OF HTPB BASED COMPOSITE SOLID
PROPELLANTS**

**A THESIS SUBMITTED TO
THE GRADUATE SCHOOL OF NATURAL AND APPLIED SCIENCES
OF
THE MIDDLE EAST TECHNICAL UNIVERSITY**

BY

CEVAT ERİŞKEN

56599

**IN PARTIAL FULFILLMENT OF THE REQUIREMENTS FOR THE DEGREE
OF MASTER OF SCIENCE**

IN

THE DEPARTMENT OF CHEMICAL ENGINEERING

JANUARY 1996

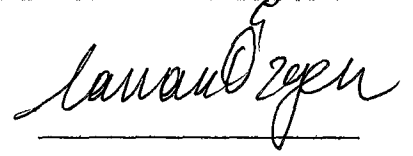
**M.Ö. YÜKSEKÖĞRETİM KURULU
DOKÜMANTASYON MERKEZİ**

Approval of the Graduate School of Natural and Applied Sciences



Prof. Dr. İsmail Tosun
Director

I certify that this thesis satisfies all the requirements as a thesis for the degree of Master of Sciences



Prof. Dr. Canan Özgen
Head of Department

We certify that we have read this thesis and that in opinions it is fully adequate, in scope and quality, as a thesis for the degree of Master of Science.



Prof. Dr. Ülkü Yilmazer
Supervisor



Prof. Dr. Saim Özkar
Co-Supervisor

Examining Committee Members

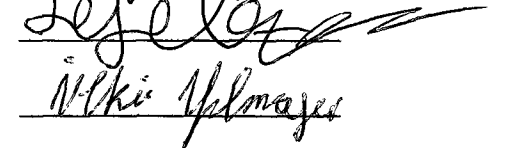
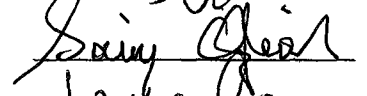
Prof. Dr. GÜNGÖR GÜNDÜZ (Chairman)

Prof. Dr. Timur Doğu

Prof. Dr. Saim Özkar

Prof. Dr. Levent Yılmaz

Prof. Dr. Ülkü Yilmazer



ABSTRACT

MODELING AND RHEOLOGY OF HTPB BASED COMPOSITE SOLID PROPELLANTS

Erişken, Cevat

M.S., Department of Chemical Engineering

Supervisor: Prof. Dr. Ülkü Yilmazer

Co-Supervisor: Prof. Dr. Saim Özkar

January 1996, 90 pages

Achievement of high density and specific impulse has been the ultimate goal of propellant development. Without changing the design of the motor the only way to get this is to increase the solid content of the propellant. Increasing the solid content, however, causes variations in the rheological as well as mechanical properties of the propellant. For a defect free casting, a propellant with minimum viscosity is required. The minimum viscosity propellant can be obtained by the proper selection of the fractions of solid component sizes leading to maximum packing density.

In this study Furnas' model was used to predict the particulate composition for the maximum packing density. Components with certain size dispersions were combined to yield a size distribution which is closest to the optimum one given by Furnas for maximum packing. The closeness of the calculated size distribution to the optimum one was tested by using the least square technique. The results obtained in this way were experimentally confirmed by rheological characterization of uncured propellants the solid part of which was prepared accordingly. Aluminum powder (volumetric mean particle diameter of 10.4μ) and ammonium perchlorate with four different sizes (the volumetric mean particle diameters: $9.22\ \mu$, $31.4\ \mu$, $171\ \mu$, and $323\ \mu$) were used in the preparation of a series of propellants having trimodal solid part and HTPB binder. In all of these propellants, the aluminum content of the solid part was kept constant for ballistic purposes. The propellant composition having maximum fluidity was determined by measuring viscosities of uncured propellants using a Brookfield Viscometer with T spindle. The experimental measurements showed that the compositions for the minimum viscosity are in good agreement with those predicted by using the model for maximum packing.

The propellant consisting of particles with mean diameters of 10.4μ , 31.4μ and 323μ was found to yield minimum viscosity. This minimum viscosity was observed when the fraction of the sizes with respect to total solids is 0.1412, 0.300 and 0.5588 respectively. The propellant with these fractions of particles was found to be processable up to 82% volume loading level.

Keywords: Modeling, Packing, Composite Solid Propellant, HTPB, Rheology

ÖZ

HTPB ESASLI KOMPOZİT KATI YAKITLARIN MODELLENMESİ VE REOLOJİSİ

Erişken, Cevat

Yüksek Lisans, Kimya Mühendisliği Bölümü

Tez Yöneticisi: Prof. Dr. Ülkü Yılmaz

Ortak Tez Yöneticisi: Prof. Dr. Saim Özkar

Ocak 1996, 90 sayfa

Yakıt performansının geliştirilmesinde en büyük hedef yüksek yoğunluk ve özgül itki elde edebilmek olmuştur. Motorun tasarımında herhangi bir değişiklik yapmaksızın bunu gerçekleştirmenin tek yolu yakıtın katı miktarının arttırılmasıdır. Katı miktarının arttırılması diğer yandan yakıtın reolojik ve mekanik özelliklerinde değişikliklere sebebiyet vermektedir. Yakıtın motorlara kolayca ve boşluk kalmayacak şekilde dökülebilmesi için yakıtın viskozitesinin mümkün olduğunca düşük olması gerekmektedir. Yakıtın katı bileşenlerinin en iyi istiflenmeyi sağlayan oranlarının tespit edilmesiyle en düşük viskozite elde edilebilir.

Bu çalışmada katı bileşenlerin en iyi istiflenmeyi sağlayan oranlarının belirlenmesinde Furnas'ın modeli kullanılmıştır. Belirli tanecik dağılımlarına sahip bileşenler, Furnas'ın geliştirdiği en iyi istiflenmeyi veren tanecik dağılımına en yakın dağılıma sahip olacak şekilde harmanlanmıştır. Hesaplanan tanecik dağılımının en iyi istiflenmeyi veren dağılıma olan yakınlığı en küçük kareler yöntemi ile ölçülmüştür. Bu yolla elde edilen sonuçlar, katı bileşen oranları bu sonuçlara uygun olacak şekilde hazırlanan yakıtlar üzerinde yapılan deneylerle doğrulanmıştır. Yakıtın üçlü-boyuta sahip katı kısmı, alüminyum tozu (hacimsel ortalama tanecik boyutu 10.4μ) ve dört farklı boyutta mevcut olan amonyum perklorat taneciklerinden (hacimsel ortalama tanecik boyutları: 9.22μ , 31.4μ , 171μ , 323μ), bağlayıcı kısmı da başlıca HTPB'den meydana gelmektedir. Balistik özelliklerden dolayı katı kısımdaki alüminyum miktarı bütün yakıtlarda sabit tutulmuştur. Hazırlanan yakıtların viskoziteleri Brookfield viskometresi kullanılarak ölçülmüş ve en iyi akışkanlığa sahip olan yakıtın katı oranları tespit edilmiştir. Deney sonuçları en düşük viskoziteyi veren katı oranlarının modelden elde edilen ve en iyi istiflenmeyi sağlayan katı oranları ile uyumlu olduğunu göstermiştir.

Hacimsel ortalama tanecik boyutları 10.4μ , 31.4μ ve 323μ olan taneciklerden oluşan yakıtın en düşük viskoziteyi verdiği görülmüştür. En düşük viskozite bu taneciklerin toplam katılar içindeki oranları sırasıyla 0.1412, 0.300 ve 0.5588 olduğu durumda gözlenmiştir. Bu oranlarla hazırlanan yakıtın hacimsel olarak %82 katı yükleme seviyesine kadar dökülebilir olduğu tespit edilmiştir.

Anahtar Sözcükler: Modelleme, İstifleme, Kompozit Katı Yakıtlar, HTPB, Reoloji

ACKNOWLEDGMENTS

I am very grateful to Prof. Dr. Ülkü YILMAZER and Prof. Dr. Saim ÖZKAR for their guidance.

I would like to thank The Scientific and Technical Research Council of Turkiye- Defense Industries Research and Development Institute for its financial support.

I also would like to thank the members of the Propellant Technologies Department of Defense Industries Research and Development Institute and the members of Chemical Engineering Department of Middle East Technical University.

Finally, my family deserves most of the thanks due to their unlimited support during my education.

TABLE OF CONTENTS

ABSTRACT.....	iii
ÖZ.....	v
ACKNOWLEDGMENTS.....	vii
TABLE OF CONTENTS.....	viii
LIST OF TABLES.....	xi
LIST OF FIGURES.....	xii
CHAPTER	
1. INTRODUCTION.....	1
2. LITERATURE SURVEY.....	5
2.1. Uncured Propellant Rheology.....	5
2.2. Factors Affecting the Rheology of Uncured Propellant....	7
2.2.1. Solid loading level.....	8
2.2.2. Packing density of particles.....	11
2.2.2.1. Modality (number of component sizes) of solids mixtures	11
2.2.2.2. Particle size and size distribution.....	15
2.2.2.3. Composition of the solid component sizes.....	19
2.2.2.4. Shape of particles.....	20
2.2.3. Effect of particulate interactions.....	23
2.2.4. Effect of temperature.....	25

2.2.5.	Other related factors in propellant rheology.....	27
3.	THEORY.....	29
3.1.	Mathematical Modeling for Obtaining Fractional Solid Content at Maximum Packing Condition.....	29
3.1.1.	Furnas' approach to the development of optimum size distribution.....	30
3.1.2.	Determination of fractional volumes of components with different sizes.....	33
4.	EXPERIMENTAL.....	36
4.1.	Experiments for Mathematical Modeling.....	36
4.1.1.	Materials and equipment.....	36
4.1.2.	Procedure for particle size measurement and void fraction determination.....	38
4.2.	Experiments for Rheological Measurements.....	39
4.2.1.	Mixing equipment and procedure.....	39
4.2.2.	Measuring equipment and procedure.....	40
5.	RESULTS AND DISCUSSIONS.....	44
5.1.	Application of the Developed Model.....	44
5.1.1.	Particle size distribution of solid components.....	44
5.1.2.	Calculation of void fractions.....	45
5.1.3.	Calculation of the fractions of the solid component sizes	48
5.2.	Results of Rheological Measurements.....	52
5.2.1.	Effect of temperature.....	57
5.2.2.	Effect of the mean diameter ratio of the solid components.....	58
5.2.3.	Effect of fractional variations of components.....	61

5.2.4.	Effect of solid loading.....	64
5.3.	Comparison of Model and Experimental Results.....	66
6.	CONCLUSIONS AND RECOMMENDATIONS.....	69
REFERENCES.....		71
APPENDICES.....		75
A.	SIZE DISTRIBUTIONS OF SOLID COMPONENTS.....	75
B.	MODEL AND OPTIMUM SIZE DISTRIBUTIONS.....	80
C.	RESULTS OF VISCOSITY MEASUREMENTS.....	83



LIST OF TABLES

TABLE

2.1. Fluidity of bimodal distributions of 55% volume suspensions of glass spheres in a water solution of zinc bromide and glycerol.....	12
2.2. Porosity-coordination number relation of spheres.....	22
3.1. Size analysis of components.....	34
4.1. Solid materials' specifications.....	37
5.1. Void fractions of component sizes.....	46
5.2. Optimum size distributions for the solid mixtures.....	51
5.3. Model results for the fractions of the solid components.....	52
5.4. The results of the viscosity measurements of the propellant slurries at different rpm's.....	60
5.5. Comparison of the model results with the experimental findings.....	66
A.1. Size distribution of 9.22 micron AP particles.....	75
A.2. Size distribution of 10.4 micron (Al) particles.....	76
A.3. Size distribution of 31.4 micron AP particles.....	77
A.4. Size distribution of 171 micron AP particles.....	78
A.5. Size distribution of 323 micron AP particles.....	79
C.1. Results of viscosity measurements at different shear rates.....	83

LIST OF FIGURES

FIGURES

2.1. Relative viscosity-concentration curve obtained by three types of viscometers.....	10
2.2. Calculated relative viscosity curves of multimodal suspensions.....	14
2.3. Effect of various particle size ratios on the flow behavior of bimodal suspensions containing 65% volume resin at 25°C.....	17
2.4. Effect of concentration on the viscosity of particles with different shapes in water at a shear rate of 327.7 s ⁻¹	23
2.5. Effect of temperature and time on viscosity index.....	26
4.1. Photograph of the 1 gallon Baker Perkins mixer.....	41
4.2. Photograph of the Brookfield Viscometer.....	41
4.3. Flowchart of the propellant manufacturing process.....	43
5.1. Variation of void fraction with mean particle diameter.....	47
5.2. Experimental verification of Equation (3.3).....	49
5.3. Time dependency of the propellant slurry viscosity.....	54
5.4. Shear rate dependency of the propellant slurry viscosity.....	55
5.5. The reproducibility of the viscosity measurements.....	56
5.6. Effect of temperature on the viscosity of the uncured propellant....	58

5.7. Effect of mean diameter ratio on the viscosity (at 2.5 rpm) of the uncured propellant.....	59
5.8. Effect of fraction of the fines in the total solids on the viscosity of the propellant slurry.....	62
5.9. Effect of fraction of the fines in the total solids on the viscosity of the propellant slurry.....	63
5.10. Variation in viscosity of the propellant with increasing total volume concentration of solids.....	65
B.1. Comparison of model and optimum distributions for Set No 1.....	80
B.2. Comparison of model and optimum distributions for Set No 2.....	80
B.3. Comparison of model and optimum distributions for Set No 3.....	81
B.4. Comparison of model and optimum distributions for Set No 4.....	81
B.5. Comparison of model and optimum distributions for Set No 5.....	82
B.6. Comparison of model and optimum distributions for Set No 6.....	82



To my Father, Mother, and Brother

CHAPTER 1

INTRODUCTION

Composite solid propellant is a heterogeneous mixture of three major ingredients, a polymeric binder, a solid oxidizer and a metallic fuel. In the manufacture of solid propellants, generally, Hydroxyl Terminated Polybutadiene (HTPB), Ammonium Perchlorate (AP) and Aluminum Powder (Al) are used as binder, oxidizer, and metallic fuel, respectively. During processing, solid ingredients are dispersed into the polymer matrix and mixed at a specified temperature for sufficient period of time to obtain a mixture as uniform as possible. The polymer matrix subjected to this process is composed of HTPB, Dioctyladipate (DOA), Triethanolamine (TEA), and TEPANOL. Because of the reactivity of the mixture and high temperature sensitivity of mixture viscosity, temperature is considered as a critical parameter during the process. Finally, a curative, Isophorondiisocyanate (IPDI), is added into the system and the propellant is transferred to a previously prepared rocket motor case.

Obtaining high levels of specific impulse and density is always the ultimate goal of propellant development, because these are the major factors affecting the performance of the rocket. As the solid content of the propellant is increased, its

density increases resulting in an increase in the specific impulse and range. Previous studies have shown that a ten percent increase in AP content (from 70% to 80% by weight) increases the specific impulse (I_{sp}) from 185 to 225 sec (Kubota, 1984). Further increase in AP content causes I_{sp} to reach a maximum value and after this particular value it shows a decreasing trend. Having an increase in the I_{sp} by increasing the solid content causes variations in the rheological and mechanical properties of the propellant. It is well known that an increase in the solid content results in an increase in the viscosity of the uncured propellant and a decrease in the percent elongation of the cured propellant, hence causing a difficulty in the processing and failure in the absorption of the stresses in the rocket motor, respectively. Therefore the solid loading should be increased to such a level that propellant still remains processable and the other properties are still satisfactory. A propellant is known as 'uncured' between the time period of the addition of curing agent and disappearance of its fluidity.

The rheology of filled liquid polymers, such as uncured solid propellants, is extremely complex from a theoretical point of view. Therefore, determination of the flow behavior of such systems from the knowledge of its individual components properties is generally not possible. Although there are works carried out to estimate the propellant flow behavior, none of them is able to determine its behavior fully. Uncured solid propellants generally exhibit non-Newtonian flow behavior, i.e., viscosity is a function of the applied shear rate. This non-Newtonian behavior of propellant is attributed to the amount of solids contained in the propellant, because the polymer matrix itself shows a Newtonian flow behavior. Clearly, the rheology of the propellant dispersion is important task in the manufacturing process.

One way to increase the solid content with a minimal change in the rheological and mechanical properties is to use the concept of packing density. Packing density is defined as the fraction of voids in a bed which is occupied by solid particles. Theory of particle packing is based on the selection of proper sizes and proportions of particulate material so that larger voids are filled with smaller particles, and the new small voids created are in turn filled with still smaller particles, and so on. It is obvious from this statement that packing density is greatly influenced by the size of particles. Solid particles used in this work are aluminum particles and ammonium perchlorate particles. The AP particles already available in hand have volumetric mean particle diameters of 9.22 μ , 31.4 μ , 171 μ , and 323 μ . The volumetric mean diameter of aluminum particles is 10.4 μ . There are other parameters affecting the density of packing, e.g. the distribution of sizes, shape and surface characteristics of particles, number of component sizes (modality), proportions of components in the mixture, mean diameter ratio of components, and interactions between particles themselves and between particles and suspending fluid. In studies with concentrated suspensions, it is found that fluidity of the suspension decreases with an increase in the solid content, but increases with an increase in the packing density at a specified solid content. The aim is, therefore, to pack as much ammonium perchlorate and aluminum particles as possible within a unit volume of propellant.

In studies of uncured propellant rheology, the aim is always to have a propellant with minimum viscosity so that, a defect free propellant casting can be achieved. Developing a model that gives the composition of particulates leading to maximum packing density will therefore be very helpful in obtaining a propellant

with minimum viscosity. An optimum size distribution leading to maximum packing density was obtained previously (Furnas, 1931) for discrete particle sizes. In the development of the present model, it is assumed that this optimum size distribution is applicable for aluminum and ammonium perchlorate particles. Based on this assumption, the model estimates the fraction of each solid component that yields a size distribution which is closest to the optimum distribution. The idea here is to minimize the deviation between the optimum size distribution and the size distribution obtained by the model. Mathematically, this idea can be expressed by a differential equation, and solution to this equation gives the fractions of components.

Verification of the developed model by rheological characterization of propellants with predetermined fractions of components is the other objective of this study. Using the sizes in hand, trimodal mixtures were prepared according to model results and propellants were manufactured accordingly. The aluminum content was kept constant for ballistic purposes. Compositions which are different from the model were also tried to observe the effect of size composition on the propellant rheology. The propellant composition having maximum fluidity was determined by measuring their viscosities using a Brookfield Viscometer with T spindle.

After determining the propellant composition with minimum viscosity both theoretically and experimentally, the third and the main objective of the work is to increase the solid loading level of this particular propellant. The loading level of the propellant was increased from 75% to 86% by volume and it was observed that propellant remains processable up to the loading level of 82% by volume. The measured apparent viscosity of the uncured propellant slurry at this loading level is 2730 poise at 2.5 rpm spindle speed which is low enough to cast.

CHAPTER 2

LITERATURE SURVEY

2.1 Uncured Propellant Rheology

A solid propellant is usually manufactured in batches by dispersing solids into the low molecular weight polymer matrix using a vertical mixer. When the mixing is complete the uncured propellant is transferred to the motor case and left at a specified temperature for a period of time for curing. The flow characteristics of uncured solid composite propellants during motor casting are important because they have a direct effect on the motor grain integrity.

Most solid propellants in an uncured state exhibit non-Newtonian flow behavior because suspensions of particles in Newtonian fluids exhibit a shear dependent viscosity at moderate and high solid concentrations. Shear dependent viscosity is a reflection of the change in the structure with shearing, e.g., breakup of agglomerates into smaller ones, change in the orientation distribution with flow strength, change in inertia of heavy particles affecting particle interactions, etc. The power law model given in Equation (2.1) is frequently used to determine the degree of shear dependency for limited ranges of shear rates (Kamal, 1985):

$$\eta = k\dot{\gamma}^{-n} \quad (2.1)$$

where η is the suspension viscosity, n and k are parameters determined from experimental data. A material such as uncured propellant, whose viscosity increases steadily as the shear rate is reduced to zero is called as a pseudoplastic material. Pseudoplasticity of the suspension is usually increased by increasing concentration of particles (Kataoka et al, 1978). However, it was reported that the power law index 'n' is independent of concentration at the high shear rate range (Mewis, 1975). The propellant viscosity may actually become infinite at some finite value of the shear rate showing the property of Bingham plastic materials.

Uncured solid propellants may also exhibit a type of flow behavior known as 'thixotropy'. A thixotropic material subjected to constant rate of shear shows a decrease in viscosity with time. Another common property of all uncured propellants is that their flow characteristics change as the cure reaction proceeds. Thus an uncured propellant may exhibit near Newtonian flow behavior shortly after the addition of the curing agent. Then as the curing reaction proceeds the flow characteristics will exhibit pseudoplastic behavior. All propellants develop pseudoplastic flow behavior after the curative addition and differ only in the rate of development of pseudoplasticity (Klager, 1978).

Since the viscosity or flow characteristics of uncured propellants are dependent on the shear rate and time, an efficient processing and casting depends on good control of these parameters. The flow behavior in the mixing process differs from the flow behavior in casting. While the propellant is subjected to a constant shear rate in the mixing process, it is subjected to high-shear rate in the casting tube

and low-shear rate in the rest of the motor. The shear rate decreases rapidly as the propellant moves away from the point where the stream of the propellant being cast enters the bulk of the propellant in the motor. After the propellant leaves the mixing zone, the flow towards the wall and to the core occurs under low applied stress, actually only under its own hydrostatic head. Under these conditions the apparent viscosity of a pseudoplastic material will be very high. The characteristics of the propellant in this zone are directly dependent on the flow processes occurring in the mixing zone. If a propellant, with a long elapsed time after the curative addition is being forced into the zone there is a high probability of existence of defects. In addition to its own hydrostatic head, propellant is subjected to vacuum draining during its transfer. As the propellant cure reaction proceeds, propellants will eventually show extreme pseudoplastic behavior. Therefore, either the time elapsed after curative addition should be decreased which is not possible due to technical requirements or new formulations should be developed as to obtain minimum viscosity propellant composition.

2.2. Factors Affecting the Rheology of Uncured Propellant

From the above section one can understand how the rheology of uncured propellant is important in mixing process and during its transfer. To be more clear, it is necessary to examine the factors mostly effective on the uncured propellant rheology.

2.2.1. Solid loading level

Rheology of concentrated suspensions has been under examination since 1950's. The very first studies on this subject were on the theoretical estimation of viscosity with changing solid concentration and the determination of maximum loading level. First studies (Roscoe, 1952) were able to predict viscosities of suspensions concentrated up to 30% volume. However, from the point of view of simplicity and usefulness over a range of concentration up to 50% volume or more, the most satisfactory relation for expressing the variation of viscosity with concentration has been that due to Maron et al. in 1951. The viscosities of suspensions consisting of uniform-size rigid spherical particles were measured by Sweeney and Geckler in 1954. This was one of the first experimental studies performed on the rheology of suspensions. In that study, a rotational (Couette type) viscometer was used to measure the suspension viscosity consisting of glass spheres as filler and fused zinc bromide in aqueous glycerol as suspending medium. They selected this pair because of their relatively close densities. They were able to measure a 55% maximum solid loading level in their work.

Chong et al. in 1971, studied suspensions with uniform-size glass beads and measured viscosity as a function of solids concentration. The solids concentration ranged from 45% to over 60% by volume, sizes from 53.8 to 236 microns, and temperature was kept at 20, 30, and 40°C. An orifice viscometer was used in the study. They concluded that, for monodispersed (unimodal) systems the relative viscosity, defined as the ratio of the suspension viscosity to the suspending medium viscosity, is independent of the particle size and temperature and is a function only

of the solids concentration. At 60.5% solids loading there existed an asymptotic behavior of viscosity indicating the occurrence of maximum loading level.

In one of the recent studies Hoffman in 1992 measured viscosities of monomodal suspensions. Suspension was composed of an acrylate rubber as the principal component in the particles surrounded by water. He used a Weissenberg Rheogoniometer, Model R16 having a flow geometry of cone-and-plate flow. He increased the loading level up to 60% volume and examined the effect of concentration on viscosity. Hoffman found that, the suspensions had a near Newtonian flow behavior at a resin level 35% by volume, but at higher levels the suspensions become strongly shear thinning in their flow behavior. Also he measured an initial relative viscosity of 8 at the concentration level of 35%, while measuring a relative viscosity of 300,000 at the concentration level of 60%. The particle diameter of this unimodal suspension was 0.21μ . At resin levels above 60% by volume, suspensions containing monosized particles showed a Bingham fluid-like behavior in that they would not flow out and form a smooth surface under the force of gravity.

The rheological behavior of suspensions has been studied widely for many years. Some authors worked on the verification of the theoretical studies and observed that theoretical or empirical relations work only at dilute or moderately concentrated suspensions. The most reliable results are, therefore, those obtained by experimental measurements. Metzner in 1985, collected experimental data obtained by different measurement techniques and compared them to make a general conclusion. The result of Metzner's work is given in Figure 2.1.

According to Metzner, i) the volumetric concentration level controls the viscosity level, ii) as concentration levels corresponding to a dense packing of solid particles are approached there is no longer sufficient fluid in the system to lubricate the relative motion of particles and as expected the viscosity increases to infinity.

Examination of the works on the rheology of unimodal dispersions shows that there is an upper limit for solid loading above which the suspension is not processable, due to infinite viscosity. When the aim is to load as much solids as possible as in the case of solid propellants, it is necessary to find some means of extending that upper limit.

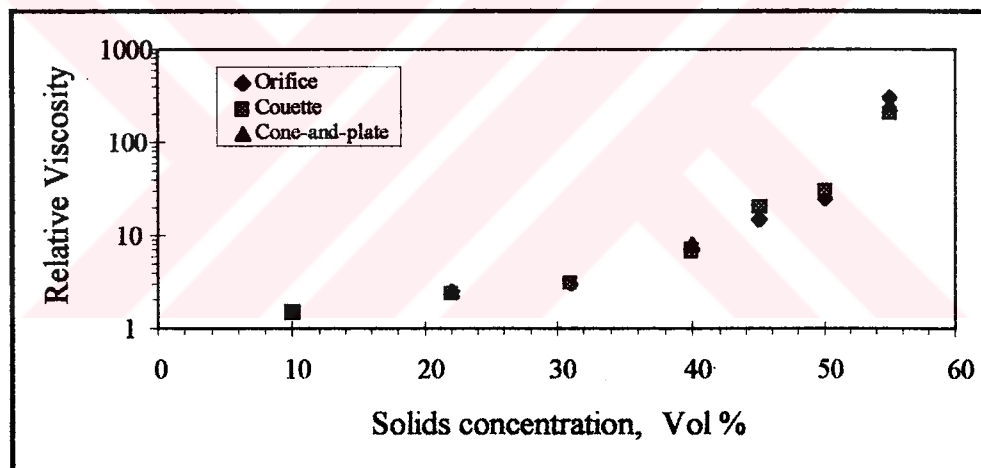


Figure 2.1. Relative viscosity-concentration curve obtained by three types of viscometers (Metzner, 1985)

2.2.2 Packing density of particles

The rheology of suspensions considering the factors affecting the packing density has been extensively studied. In general, the viscosity of suspensions decreases with increasing packing density. In the estimation of minimum viscosity, determination of solids fractions giving maximum packing density can be studied by dry mixing. In some cases, however, especially when non-uniform, irregular shaped, and interacting particles are encountered the results of dry mixing are not sufficient for a good estimation. A preliminary study was performed to estimate the packing density of aluminum and ammonium perchlorate particles by dry mixing. But, the results did not show good agreement with the previously obtained data.

Factors affecting packing density indirectly affect the rheology of suspensions and it is therefore necessary to examine these factors individually.

2.2.2.1 Modality (number of component sizes) of solids mixtures

It is known that the limiting concentration of filler in a suspension can be increased by increasing modality. Sweeney and Geckler, in 1954, carried out experiments at constant (55%) volumetric loading with bimodal glass spheres to examine the effect of modality on fluidity. The experimental parameters and their results are given in Table 2.1. The first row in the table corresponds to the suspension of unimodal particles and the rest to the suspensions of bimodal particles. It is seen that the fluidity of the suspension increases when the modality is increased

from unimodal to bimodal. The suspension has a fluidity of 0.00958 poise⁻¹ when it is composed of unimodal particles while having a fluidity of 0.0415 poise⁻¹ with bimodal particles. However, this trend is not as expected in the second row. This indicates that modality is not the only factor affecting the fluidity of a suspension.

Table 2.1. Fluidity of bimodal distributions of 55% volume suspensions of glass spheres^a in a water solution of zinc bromide and glycerol^b(Sweeney and Geckler, 1954).

Diameter of small spheres (microns)	Volumetric mean diameter of small spheres (microns)	Diameter ratio of small to large spheres	Apparent fluidity at rest (poise ⁻¹)	Apparent fluidity at infinite shear stress (poise ⁻¹)
239-282	261.6	1.000	0.00958	0.0182
147-177	164.0	0.627	0.0077	0.0168
88-105	97.0	0.371	0.0129	0.0213
20-45	35.9	0.137	0.0229	0.0223
<20	12.6	0.048	0.0415	0.0310

^a Glass spheres consisted of 75 percent of 239-282 micron diameter and 25 percent of diameter shown in first column.

^b Suspending medium: density 2.494 g.cm⁻³, fluidity 0.3701 poise⁻¹

There have been also theoretical approaches for the estimation of viscosity of multimodal suspensions from unimodal viscosity data. This assumes no interactions between particles. This assumption was confirmed by Fidleris and Whitemore (1961) who investigated the settling velocity of a large sphere in a 20% suspension of uniform-sized small spheres. The results of their investigation showed that if the size ratio (small to large) is 1/10 or less, then the small spheres behave as a fluid in

the suspension. When the size ratio becomes greater than 1/10 the falling sphere follows a zig-zag random path instead of a linear path.

Based on the results of Fidleris' work, Farris, in 1968, developed a model predicting the viscosities of multimodal suspensions. He derived a relation as:

$$\ln \eta_r = \sum_{i=1}^N \ln H(\Phi_i) \quad (2.2)$$

where η_r is the relative viscosity of the suspension compared to the pure liquid, $H(\Phi)$ is the ratio of the viscosities of the two succeeding filled suspensions ($H(\Phi) >$

1). If the mixture is composed of five different sizes, for example, $H(\Phi_5)$ is the ratio of the viscosity of suspension after the addition of the fifth size, to the viscosity of tetramodal suspension. He also derived the following relation for the total filler concentration as a function of the concentrations of each component size.

$$(1 - \Phi_T) = \prod_{i=1}^N (1 - \Phi_i) \quad (2.3)$$

In above equation, N is the number of component sizes, Φ_i is the fraction of each component and Φ_T is the total filler concentration which is defined as:

$$\Phi_T = \frac{\sum_{i=1}^N V_i}{\sum_{i=0}^N V_i} \quad (2.4)$$

Because all the above relations are particle diameter independent, Farris' work underestimates the effect of diameter ratios (smallest to largest) when this ratio is greater than 1/10 and can only be used to observe the effect of modality for a predetermined set of particles. Using these relations, Farris calculated the viscosities of multimodal suspensions at different filler concentrations. The results of these predictions are given in Figure 2.2 by curves which allow one to compare the multimodal systems. Considering these results, one may conclude that a trimodal distribution would be helpful in reducing the viscosity level if the loading level exceeds 50%. This reduction in viscosity is greatest when the modality is changed from unimodal to bimodal and it becomes insignificant after trimodal. Metzner (1985) gives theoretically calculated relative viscosities of unimodal, bimodal, trimodal and tetramodal suspensions as 1200, 51, 30, and 23, respectively.

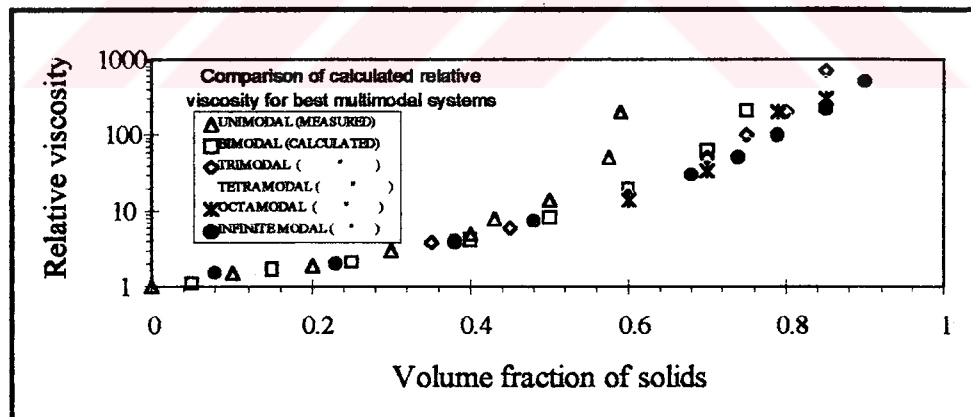


Figure 2.2. Calculated relative viscosity curves of multimodal suspensions (Farris, 1968)

2.2.2.2. Particle size and size distribution

By using multimodal sizes, the limiting solids content can be increased considerably, but the size ratios should also be determined experimentally. Although not considered by Farris, the effect of diameter ratio has been the subject of many studies since the experimental study of Sweeney and Geckler (1954). They measured the fluidity of suspensions with various diameter ratios at a particular composition of small and large spheres. It was found out that the suspension with 20 and 260 micron particles has maximum fluidity (See Table 2.1). Furthermore, the initial viscosity of the bi-disperse system with above conditions has been decreased 4.3 times over that of the monodisperse system with large spheres. It is a direct result of this study that in addition to modality, the rheology of suspensions is also affected by the smallest to largest diameter ratio of the fillers.

Chong et al. in 1971 carried out experiments with glass spheres having diameter ratios of 0.477, 0.33, and 0.138 which are above the critical ratio of 0.1. In their work, the solid loading was increased from 54% to 74% by volume at above given diameter ratios, keeping the amount of small spheres constant at 25%. Their results showed that, the viscosity of suspension increases with increasing loading level as expected. When their data are plotted on a semi-log graph it is easily seen that as the diameter ratio (small to large) approaches 0.1, at a particular loading level the viscosity of suspension decreases. This is an indication of the fact that, as the ratio (small to large) of particles gets smaller, a better packing is achievable and the viscosity of suspension decreases.

The effect of particle diameter was also studied by Hoffman (1992). He increased the loading level from 35% to 60% by volume for suspensions with particles having different diameters and measured the relative viscosity. At the loading level of 35%, both suspensions with 0.21μ and 0.95μ particles had a relative viscosity of 8 approximately. When the loading was increased to 60%, however, the relative viscosity of suspension of 0.21μ particles became 300,000 while that of 0.95μ particles increased only to 5000. He deduced from these results that, at high loading levels the effect of colloid chemical forces increases due to the decrease in the particle size and the space between them. Measurements made with different particle diameters (0.27μ , 0.68μ , and 0.95μ) showed that, in the range studied the particle size is not important at the loading level of 35% volume, but the particle size becomes quite important when the volume percent of the solids is as high as 55%.

Similar to Chong et al. (1971), Hoffman studied the effect of diameter ratio of the bimodal suspensions at a loading level of 65% volume. The size ratios he considered were 0.4, 0.3125, and 0.147 which are above the critical ratio of 0.1. Results of his experimental measurements are given in Figure 2.3. In this study, Hoffman observed that the diameter ratio of the particles is very important, and among the sets of particles, combination of particles with a diameter ratio of 0.147 gives the smallest viscosity. Knowing the diameter ratio of particles alone, however, is not sufficient for claiming that the viscosity of the suspension is minimum. Figure 2.3 shows that at a particular fraction (0.8) of large component, suspension having the smallest diameter ratio of 0.147 has the smallest relative viscosity among the viscosities of the suspensions.

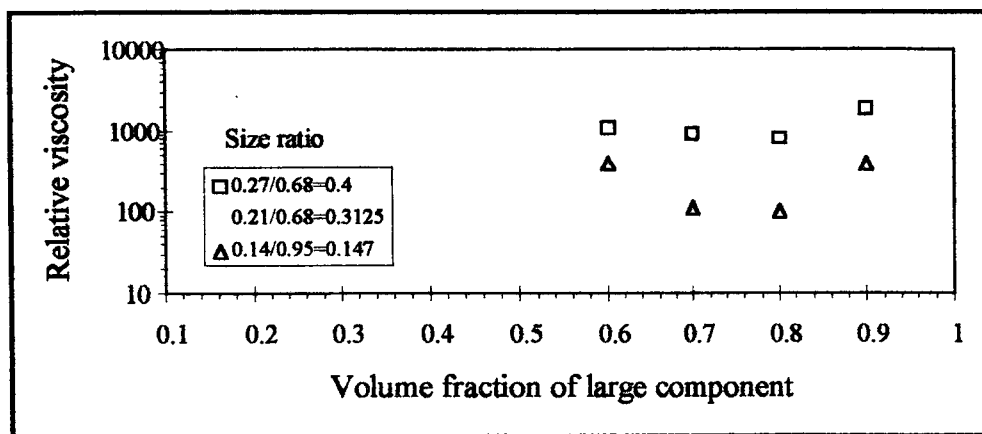


Figure 2.3. Effect of various particle size ratios on the flow behavior of bimodal suspensions containing 65% volume resin at 25°C (Hoffman, 1992)

All the studies given so far are related to suspensions consisting of mixtures with two unimodal particles of uniform sizes. These are very ideal cases and rarely encountered in industrial applications. In real applications, particles are not uniform in size but have a continuous distribution of sizes as in the case of solid propellant technology. Fine sizes of ammonium perchlorate are obtained by grinding the larger sizes and it is not possible to get uniformly sized particles. It is, therefore, necessary to know how the rheology of suspensions is affected by the distribution of sizes. Hoffman, actually, used non-uniformly sized particles, but the ranges of sizes were (0.75-1.2 μ and 0.1-0.6 μ) too narrow to observe this effect.

An illustrative work on this field was performed by Probstein et al. in 1994. To avoid the effect of colloidal particles they introduced large particles into the suspension. The suspending medium was a zinc bromide solution. The particles used were of two types. One was uniformly distributed (in the range 35-200 μ) and the other was log-normally distributed in the same range. Viscosities of the two

suspensions containing these particles were measured up to 50% volume solid loading level. The results did not show very much difference between the measured viscosities at low concentration levels. However, at the concentration level of 50% solids, the measured viscosity of the suspension with log-normally distributed particles is twice of the measured viscosity of the suspension with uniformly distributed particles.

The effects of continuous distribution of particle sizes on the rheology of suspensions necessitate more examination due to their extensive application. The effect of continuous distribution of particle sizes on the packing density, rather than the rheology, has been studied for years. Following the theoretical study of Furnas(1931), Anderegg (1931) applied his formulas to mortars and obtained relatively good agreement. The particle diameters were, however, very large (in the order of cm) as compared to the diameters considered in the present study which are measurable in microns.

Sohn and Moreland in 1968 investigated the effect of particle size distribution on the packing density of multi-particle systems. They worked with sands having particle sizes between 0.07 and 8.0 mm. Packing densities of binary mixtures of continuously distributed systems were found to depend on the packing density of each component itself, the mean size ratio of the components, and upon the composition of the mixture. They also found that, the mean particle size does not significantly affect the packing density. However the packing density is strongly affected by the dimensionless standard deviation of particle size which defines the extent of distribution. The packing density of a multi-particle system was found to increase if the particle size distribution is large.

2.2.2.3. Composition of the solid component sizes

Maintaining reasonable levels of viscosity in concentrated suspensions of multimodal particle sizes is possible by selection of proper fractions of available sizes. Compositional effect of solid components on the rheology of suspensions is as important as the modality and mean size ratio of particles used. The effects of blending regularly shaped particles is well known. Because this effect is strongly dependent on particle characteristics, specific studies are required to know the behavior of irregularly shaped particles.

The first theoretical study for the determination of relative proportions for obtaining minimum viscosity was carried out by Farris in 1968. To optimize the filler composition in a multimodal system (assuming no or equal interaction) all that is necessary is to differentiate Equation (2.2) with respect to Φ_i and set the differential equation to zero. Farris applied this to a tetramodal mixture and tabulated the relative fractions of components with different sizes for solids loading between 64% and 90% by volume. He did not consider the effect of particle diameter in this calculation.

Effect of filler composition of bimodal glass spheres was observed experimentally by Chong et al. in 1971. The optimum filler composition was determined by considering fillers with different mean diameters and solid loading levels. The relative viscosity of suspension having a diameter ratio of 0.048 first decreased up to the 40% volume of small spheres and then increased with the increasing amount of small particles. Also, large variation in viscosity was found to occur with a small change in the suspension composition at a given loading level.

Similar studies with spherical particles were performed by Poslinski et al. in 1988, Metzner in 1985, and by Hoffman in 1992. A more realistic study in this field is due to the work on the rheology of propellants carried out by Muthiah et al. in 1992. They used a mixture of HTPB prepolymer, dioctyl adipate (DOA), trimethylolpropane (TMP), and toluene diisocyanate (TDI) as the suspending medium and aluminum powder (10μ on the average), coarse ammonium perchlorate (310μ on the average), and fine ammonium perchlorate (43μ on the average) as solids. Keeping the Al content at constant level (18% weight of propellant), fraction of fine and coarse ammonium perchlorate was varied. At the weight ratio of 25/75 (fine to coarse), they measured a minimum thixotropic index which is a measure of the energy for the destruction of the thixotropic structure.

2.2.2.4. Shape of particles

The effect of shape of particles is difficult to analyze by rheological measurements. Studies on this subject are, therefore, based on the packing properties of particles. Studies on the packing of solid particles have been with spherical or near spherical particles. When the particles are uniformly sized spheres, their mode of packing is easy to define. A packing is known as 'very loose random packing' if the voidage is about 0.44, 'loose random packing' if the voidage is about 0.4, 'poured random packing' if the voidage is about 0.39, and 'close random packing' if the voidage is 0.36 (Haughey, 1969).

It is convenient to consider regular packing as assembled from layers and rows. The fundamental unit is a row of contacting spheres. These rows can be arranged parallel to each other to form a layer. The assembly of particles of this type form stable packings known as cubic, ortho-rhombic, tetragonal-sphenonoidal and rhombohedral packings. Rhombohedral is the most stable with sufficient points of contact to provide lateral stability. In contrast, cubic packing is stable only to forces perpendicular to unit cell faces and thus possesses a critical stability as observed in all the other intermediate forms.

Random packings are formed when the particles remain in position as soon as they come into contact with packing. Unlike the unique positioning of each sphere in a regular packing, the location of any sphere in a random packing can only be expressed by a probability distribution.

The points of contact between a given sphere and the adjacent spheres and the angular distribution of these points are also of interest. For regular packings, the number of such points, the coordination number, indicates the type of packing. Cubic, ortho-rhombic, tetragonal-sphenonoidal, and rhombohedral packings have respectively 6, 8, 10, and 12 contact points, each corresponding to a characteristic bulk mean voidage. Table 2.2 lists the corresponding values of voidage with respect to coordination number. It can be generalized that the coordination number of an assembly of spherical particles is a measure of packing density. Although such a correspondence between porosity and coordination number does not occur in random packings, a range of values of the coordination number is found for each mode of packing.

While many granular particles such as sand may be assumed to behave as spheres, other materials such as solid fuels, manufactured catalyst carriers, and industrial fillers form packings whose properties deviate from those of spheres.

For spherical particles the change in viscosity with respect to solid loading may be independent of particle diameter (See Figure 2.1). It is not possible to obtain a general relative viscosity-concentration curve for anisodiametric systems due to their complex and incomparable rheological behavior. Generally, the relative viscosity of fiber suspensions shows a linear dependence on concentration at very low concentrations, and nonlinearity starts at lower concentrations, as compared to suspensions of spheres, because of lower packing efficiencies. Relative viscosities at the same concentration are higher in case of fibers compared to spherical particles, as shown in Figure 2.4.

Table 2.2. Porosity-coordination number relation of spheres (Gray, 1968)

Porosity, percent	Coordination number
77.0	3
66.0	4
59.7	5
43.9	7
32.0	9
28.2	11

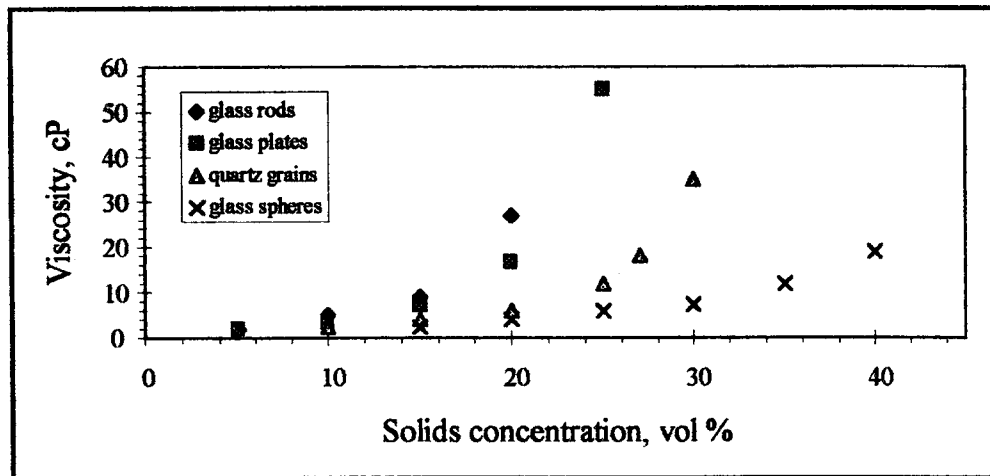


Figure 2.4. Effect of concentration on the viscosity of particles with different shapes in water at a shear rate of 327.7 s^{-1} (Kamal and Mutel, 1985)

2.2.3. Effect of particulate interactions

Particles suspended in Newtonian fluids cause additional viscous dissipation during flow and higher viscosities are observed compared to the suspending fluid itself. Rheological behavior of the system is then affected by the structures generated by particle interactions causing redistribution of particles and their orientation. The non-Newtonian behavior exhibited by suspensions of particles in Newtonian fluids can be the result of several factors influencing the suspension:

i) Non-hydrodynamic forces: Brownian forces, electrical forces arising from the charges on particles, London-van der Waals forces. Non-hydrodynamic forces are dominant in concentrated suspensions of colloidal particles (particles smaller than 1μ) and the rheological behavior of the suspension is determined by the competition between non-hydrodynamic and hydrodynamic forces yielding a viscosity which is a

function of the flow strength. Yield stresses are usually observed for concentrated colloidal suspensions due to the structures created by interparticle forces. Hoffman in 1992 carried out experiments to see the effects of both non-hydrodynamic interactions (colloidal forces) and hydrodynamic interactions on the suspension viscosity. He concluded that in concentrated dispersions of colloidally stable submicron particles, the volume fraction of particles, the particle size, and the particle size distribution are all important factors in determining the flow behavior of these systems. The importance of non-hydrodynamic forces decreases with increasing size. Generally, for suspensions of particles greater than 10μ the rheological behavior is mainly determined by hydrodynamic forces.

ii) Particle interactions: These interactions can be examined under two categories: one being the hydrodynamic interactions and the other direct particle-particle interactions. When hydrodynamic interactions between particles constitute the only factor influencing the viscosity, viscosity of the monosized suspension depends only on the concentration of particles. For multimodal suspensions, on the other hand, the viscosity is affected by the size and weight ratios of the particles (Hoffman, 1992). Particle-particle interactions are present mainly due to flocculation or aggregation of particulates. A review of the role of colloidal forces in the rheology of suspensions was made by Russel in 1980 and flocculation of particles was studied both theoretically and experimentally. Suspensions of well characterized monodisperse spheres in Newtonian fluids under steady-state conditions were analyzed and it was seen that even under these conditions the rheological behavior varies widely.

Other factors causing non-Newtonian behavior are:

- iii) Inhibition or promotion of structures by the flow
- iv) Change in particle orientation distribution with the flow strength

2.2.4. Effect of temperature

One of the most obvious factors that can have an effect on the rheological behavior of a material is temperature. Some materials are quite sensitive to temperature, and a relatively small variation will result in a significant change in viscosity. Consideration of the effect of temperature on viscosity is essential in the evaluation of materials that will be subjected to temperature variations in processing. The viscosity of the polymer matrix of the propellant, for example, is highly temperature dependent. The viscosity of the major liquid ingredient (HTPB) of the propellant decreases from 500 to 10 Poise when the temperature is raised from 0 to 65 °C. This change in viscosity is expected to be much higher when this polymer is filled with solid particles. The processing temperature of filled polymers is therefore very critical and should be controlled carefully.

When the suspension under consideration is undergoing a temperature dependent chemical reaction, the effect of process temperature gains more importance. This is exactly the case in the manufacture of solid propellants where control of temperature is very critical due to cure reaction after the addition of isocyanate. In the absence of curing agent, the propellant slurry shows a shear thinning flow behavior, i.e., the viscosity decreases with increasing shear rate. Cure reaction begins with the addition of curing agent, causing an increase in the viscosity

of slurry at the same rate of curing. Here, the trade-off between temperature and potlife is critical, since increasing the mixing temperature decreases the viscosity but increases the rate of cure. The effect of temperature on the viscosity of uncured solid propellant was studied by Osgood in 1969. He used a Brookfield Viscometer with T spindle to measure the viscosities at temperatures of 80, 100, 120, 140, and 160 °F at different aging times. The results of his measurements are given in Figure 2.5. In that figure, the viscosity index and pseudoplasticity index are, respectively, the constant and the exponent of the equation of a power law fluid.

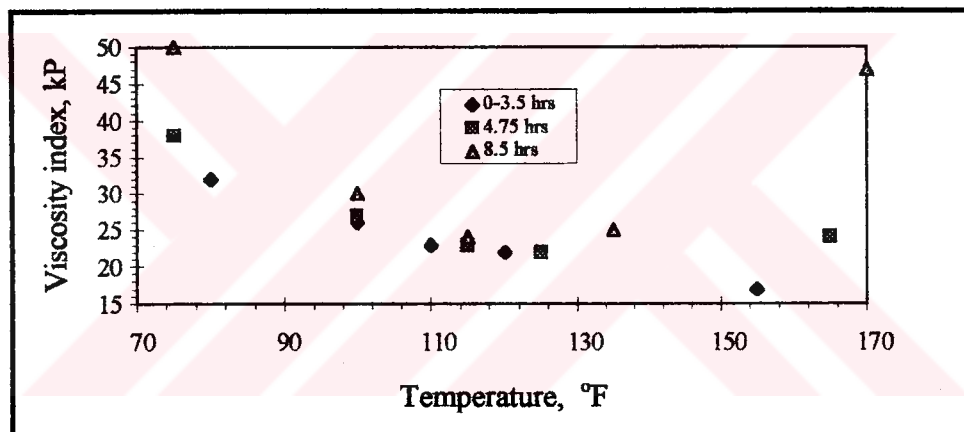


Figure 2.5. Effect of temperature and time on viscosity index (Osgood, 1969)

In 1982 Hadhoud et al. made similar measurements on uncured HTPB based propellant by using a Brookfield Viscometer. No change in the viscosity up to 120min after the addition of curative was observed but it exhibited an exponential increase after that time. They also observed that an increase in temperature from 60 to 80 °C causes the viscosity of the system to decrease from 240 poise to 40 poise.

Recently the effect of temperature on the rheological behavior of HTPB propellant slurry was studied by Muthiah et al. in 1991. A propellant slurry with 86 weight percent total solid loading having a fixed aluminum content and coarse to fine oxidizer ratio has been used to study the effect of temperature. In the temperature range of 40 to 90 °C, changes in yield stress, pseudoplasticity index, and in thixotropic index were observed. They also observed the changes in these parameters with respect to time. The conclusions they withdrew from the results are: i) the propellant slurry shows nearly time independent non-Newtonian behavior immediately after curative addition at all temperatures ranging from 40 to 90 °C, but as the cure reaction proceeds the flow becomes more and more time dependent. The thixotropic index can be considered as a parameter to represent this time dependency. ii) the fluidity of the slurry increases with temperature immediately after curative addition, but decreases as cure reaction proceeds. The slurry is reasonably flowable up to 5 h after curative addition at about 50 °C.

2.2.5. Other related factors in propellant rheology

The most important factors affecting the rheology of uncured propellant slurries have been given in the previous sections. The factors which are not very significant when considered individually, but gain importance as they come together should also be taken account in the rheological studies. These factors can be divided into two:

i) **Compositional variables:** burning rate additive type and content, bonding agent type and content, surface active agents (Landel et al., 1965), plasticizer type and content, curing agent type, cure catalyst type, trace impurities.

ii) **Processing variables:** rate and duration of mixing, extent of deaeration, efficiency of deaeration, order of addition of ingredients, mixer size and design.



CHAPTER 3

THEORY

3.1. Mathematical Modeling for Obtaining Fractional Solid Content at Maximum Packing Condition

One of the problems in packing of particles is the determination of optimum size distribution for maximum packing density. Over the years there have been many attempts to solve this problem quantitatively. Generally speaking, the early studies were largely focused on the development of optimum size distribution, without paying much attention to the determination of the fractions of multicomponent mixture. The first theoretical approach for the development of optimum size distribution was due to Furnas in 1931. His work is valid for multicomponent mixtures with continuous size distribution. Following this work, the factors affecting the packing density were studied in detail by several investigators. McGeary in 1961 extended the study of idealized packing of spheres of different sizes initiated by Furnas. The spheres he used, however, do not have continuous distribution of sizes. He performed binary, ternary, and quaternary packing of spheres experimentally and obtained 80%, 89.8%, and 95.1% of theoretical density, respectively. Sohn and Moreland studied the effect of particle size distribution in 1968, and Haughey and Beveridge(1969) made a review on the

structural properties of packed beds. Messing and Onada (1978) reviewed the subsequent experimental packing studies for specific volumes (defined as the inverse of apparent density) of mixtures and observed significant deviations from the ideal cases predicted by Furnas. One possible explanation for the discrepancy is that real multimodal powders are never perfectly mixed in dry mixing, and the local compositions vary from position to position. Assuming that the theory of Furnas adequately predicts the specific volume for a small volume element, Messing and Onada calculated the overall specific volume by summing up the contributions of every volume element in the body. They also tested this theoretical study by experiments and obtained good agreements.

Although the Furnas' theory was shown to have discrepancies when compared with experimental results of dry mixtures, it can yield good results when applied to a solid mixture wetted with a polymer matrix. To see whether Furnas' theory is applicable to such systems, it is necessary to first determine the optimum size distribution by his theory.

3.1.1. Furnas' approach to the development of optimum size distribution

The packing density of a system is known to increase with increasing number of component sizes (modality). Since a system which consists of only a few component sizes displays maximum packing for certain fractions of sizes, it may be expected that a maximum packing would also be obtained when the number of component sizes becomes very large. When the sizes are distributed, there is a

certain ratio between the two selected consecutive sizes. This ratio is taken between 1 and 1.5 for simplicity, because the ratio between the two consecutive standard screens is $\sqrt{2}$ as far as the diameter of openings is concerned. In this work, this consecutive size ratio has been taken as 1.21 due to the output of particle size analyzer. Another ratio, r , is assigned to represent the ratio (large to small) of the amount of materials on two consecutive screens. Here, the amount refers to the true volume of particles and measurement by weight is valid as long as the true specific gravity is constant from size to size. The following expression is given by Furnas (1931) for the calculation of 'r'.

$$r^{\binom{m-1}{n-1}} = \frac{1}{V} \quad \text{or} \quad r = \frac{1}{V^{\binom{n-1}{m-1}}} \quad (3.1)$$

where n : number of component sizes

m : number of screens with size ratio of 1.21

V : compositional average of the void fractions of component sizes

It is clear that the void fraction of each component size should be determined either theoretically or experimentally before beginning to develop the optimum size distribution for maximum packing density. After setting up the basic relation, the procedure for the determination of optimum particle size distribution that gives maximum packing can be explained as follows:

1. Select the size range to be used and obtain the screen sizes differing by a ratio of 1.21

2. Decide the number of component sizes, n, to be used
3. For the ratio of weight or volume in a continuous series for particles having the same true density,

$$r = \frac{1}{V^{\left(\frac{n-1}{m-1}\right)}}$$

4. For the finest size take the amount of material as 1, and for succeeding sizes obtain the amounts by multiplying previous amount by a factor r.
5. Calculate packing fraction in the continuous distribution:

$$Pf = 1 - \frac{r^{\log d} - r^{\log d_s}}{r^{\log d_l} - r^{\log d_s}} \quad (3.2)$$

where; d: ratio of sizes, 1.21

d_s : diameter of smallest particle size

d_l : diameter of largest particle size

r: ratio or factor of the amounts of sizes from step 4

Procedure described above is very helpful in determining the optimum distribution of particles for maximum packing and is used as a criterion in packing applications. Following this procedure yields a cumulative distribution of sizes.

In the studies of packing of multicomponent mixtures, Furnas' work is not the only one giving the optimum size distribution for maximum packing. Yu and Standish in 1992 proposed a method which was initiated by Fuller and Thompson

(1907). The method yields an empirically optimum cumulative particle size distribution for maximum packing. Due to its complexity in the application and since it is valid for particles having diameters of tens of millimeters, this method was decided to be improper for the present study.

3.1.2. Determination of fractional volumes of components with different sizes

Furnas' method is a good way of approaching the maximum packing value and optimum size distribution, yet it does not explain how to prepare a mixture that will yield maximum packing. It is all right if one is planning to use 'm' number of fractions and all the fractions have particles which are uniform in size. If this were the case one would take the amounts determined by the ratio 'r' and mix them for a sufficient period of time to get the maximum attainable packing. When the number of component sizes is not equal to 'm' and they are distributed over a range, however, preparation of mixture becomes somehow difficult. Furnas actually gives a plot of the number of the fractions versus the ratio of the diameter of smallest particle to the diameter of the largest particle. Using this plot he determines the number of component sizes to be combined. However, one may desire to use as many fractions as possible or the ratio of diameters may not fall in a reasonable range. It was therefore assumed that the method of determination of fractional solid content is applicable to a system of 'n' fractions but in this study only $n=3$ will be considered.

Table 3.1. Size analysis of components

Particle diameter	Size distribution of components (cumulative percent undersize)					Optimum size distribution	Size distribution of the model
	(D)	F ₁ (D)	F ₂ (D)	F ₃ (D)	F ₄ (D)		
D ₁	F ₁ (D ₁)	F ₂ (D ₁)	F ₃ (D ₁)	F ₄ (D ₁)	F _n (D ₁)	O(D ₁)	F(D ₁)
D ₂	F ₁ (D ₂)	F ₂ (D ₂)	F ₃ (D ₂)	F ₄ (D ₂)	F _n (D ₂)	O(D ₂)	F(D ₂)
.
.
D _m	F ₁ (D _m)	F ₂ (D _m)	F ₃ (D _m)	F ₄ (D _m)	F _n (D _m)	O(D _m)	F(D _m)

Referring to Table 3.1, ‘m’ is the number of screens with size ratio of 1.21, ‘n’ is the number of fractions, and ‘O(D)’ is the optimum cumulative distribution function obtained from step 4 given in the previous section.

For any given number of fractions, x_n (n=1,2,3), there is a corresponding cumulative percent distribution of the mixture which can be written as

$$F(D) = \sum_{n=1}^3 x_n F_n(D) \quad (3.3)$$

where $F_n(D)$ is the cumulative size distribution of component ‘n’ under particle size D (See Table 3.1). Equation (3.3) gives the model cumulative percent undersize corresponding to the same screen number in the optimum case. Equation (3.3) should be equal to O(D₁) for first screen, to O(D₂) for the second and so on, if there is no deviation from the optimum size distribution. It is clear that the model particle size distribution should be as close to the optimum one as possible for the packing

density to have the maximum attainable value. Thus, the difference between the optimum and the model cumulative size distributions corresponding to each screen or, for mathematical purposes, the square of the difference should be determined. Mathematically this can be expressed as

$$S = \sum_1^m [F(D_m) - O(D_m)]^2 \quad (3.4)$$

This equation contains, for this particular situation, three unknowns x_1 , x_2 , and x_3 which are the fractional volumes to be combined. It is, in general, valid for any number of fractions. To solve Equation (3.4) for values of x_n 's that make the deviation from the optimum size distribution minimum, it is necessary to differentiate the equation with respect to x_n 's and set it equal to zero, that is,

$$\frac{\partial S}{\partial x_1} = 0 ; \quad \frac{\partial S}{\partial x_2} = 0 ; \quad \frac{\partial S}{\partial x_3} = 0 \quad (3.5)$$

Fractional volumes can be obtained by simultaneous solution of the above differential equations with simple mathematical tools.

CHAPTER 4

EXPERIMENTAL

4.1. Experiments for Mathematical Modeling

4.1.1. Materials and equipment

The solid particles used in the experiments are the same as those used in manufacturing of solid propellants. These are aluminum particles and ammonium perchlorate particles with different mean diameters. All particles used in the experiments were purchased from various suppliers. The specifications of the materials are given in Table 4.1.

The equipment used for the measurements are:

- **Malvern Mastersizer Model MSX with Dry Powder Feeder Model MSX 64** for particle size measurement. This instrument is able to measure the particle sizes in the range 0.1-600 μ with an accuracy of $\pm 2\%$ with respect to volume median diameter. Malvern Mastersizer has three focal length lenses, 45 mm,

100 mm, 300 mm. The difference in the focal lengths is due to their range of application. 45 mm lens measures particles in the range 0.1-80 μ , 100 mm lens measures particles in the range 0.48-180 μ , and 300 mm lens measures particles in the range 1.2-600 μ . The instrument uses He-Ne Laser (633 nm wavelength) transmitter.

- **Heinz Janetzki K.-G. T-5 Centrifuge** for compressing the particles to leave as low voids as possible. This instrument is portable (12 kg) and can be operated on any horizontal and smooth surface. The centrifuge has four cylindrical sample units. For simplicity in application, four cylindrical tubes were prepared for these units. The tubes are 23 mm in inner diameter and 90 mm in height and the bottom of tubes are rounded. The tube diameter is recommended to be at least ten times that of the particle diameter for efficient compressing. This centrifuge can be operated at three different rotational speeds of 1000, 3000, and 5500 rpm.
- **Heating Oven** for removing any possible moisture to prevent agglomeration

Table 4.1. Solid materials' specifications

Raw material	Density (gr/cm ³)	Volume mean diameter (micron)	Specific surface area (m ² /gr)	Manufactured by
Aluminum	2.7	12	not available	Alcan Toyo
AP	1.95	40	0.330	SNPE France
		200	0.140	
		400	0.088	

4.1.2. Procedure for particle size measurement and void fraction determination

Before each measurement is taken, samples are dried in the oven at 110°C. This temperature is high enough for moisture to evaporate and low enough for AP and Al stability (AP decomposition initiates at 150°C(Kishore, 1979), melting point of Al is 660.37 °C(Weast, 1974)). Sufficient amount of sample (≈ 25 gr.) is put in the feeder of particle size analyzer and dispersed into the channel by vibrating the feed container. Vacuum suction is applied to withdraw the dispersed particles. Measurements are made by using two focal lenses. The aluminum and ground AP particles are analyzed using 100 mm focal length lens and others using 300 mm focal length lens. When the measurements are complete, the results of size distributions are displayed on the monitor and printed by a printer. The size distribution of ammonium perchlorate particles and aluminum particles are given in Appendix A.

The void fractions of samples are determined by compressing the particles in the centrifuge. Solid particles to be analyzed are first dried in the oven at 110°C before measurements are taken. Eighty grams of dried sample from one selected size is transferred into the tubes in equal amounts and the top surfaces of the samples are smoothed for ease of leveling. The tubes are then inserted into cells of the centrifuge and rotated with a speed of 5500 rpm for 15 minutes. After this period of time, the tubes are taken out and the level of the sample is marked. The apparent volume of particles is then determined by filling the tubes with distilled water, with the aid of a burette, up to the marked level of particles. The same procedure is repeated for other component sizes.

4.2. Experiments for Rheological Measurements

This part includes the mixing process of the propellant beginning by the addition of the liquid binders, followed by introduction of the solids and ending with the addition of the curing agent. Measurement of the viscosity of the propellant slurry is also included in this part. Viscosity measurements were carried out according to ASTM Standards Designation: D 2196-81.

4.2.1. Mixing equipment and procedure

Mixing process is carried out in a 1 gallon Baker Perkins vertical propellant mixer. The material of construction of the whole mixer is ex-proof stainless steel. This prevents the possibility of an explosion which may be caused by a spark due to friction. The speed of the mixer blades can be adjusted to four different rates, 15 rpm, 25 rpm, 30 rpm, and 45 rpm depending on the speed requirements. The movable container of the mixer is lowered and elevated by means of compressed air. The mixer is connected to a vacuum pump and the points of contact between the movable container and its stationary head are sealed to prevent air leakage when operated under vacuum. The vacuum pressure is 650 mmHg. Control of temperature is critical during the process due to reactions taking place. Hot water is circulated through the jacket of the mixer so that the suspension is kept at a temperature of $65\pm 1^{\circ}\text{C}$. Temperature is read from a digital screen which displays

the suspension temperature sensed by a thermocouple inserted to the inner wall of the mixer. A photograph of the mixer is given in Figure 4.1.

First the liquids are mixed to obtain uniform concentration throughout the mixture. Then aluminum and ammonium perchlorate particles are added and mixed for sufficient period of time. Finally the curative is added. The temperature is kept constant at $65\pm 1^{\circ}\text{C}$ throughout the process. When mixing is complete, a sample of propellant slurry is taken for viscosity measurements and the rest is cast for analyzing other properties. The flowchart of the process is given in Figure 4.3.

4.2.2. Measuring equipment and procedure

The instrument is a rotational type digital Brookfield Viscometer Model HBTDV-II. It measures the torque required to rotate an immersed element (the spindle) in a fluid. The spindle is driven by a synchronous motor through a calibrated spring, the deflection of the spring is indicated by a digital display. By using multiple speed transmission and different geometry of spindles a variety of viscosity ranges can be measured. When making a measurement with Brookfield Viscometers, the viscometer model, spindle type, rotational speed, container dimensions, sample temperature, and the number of spindle revolutions should be stated clearly to ensure the reproducibility of the test results. T-A spindle is the most suitable one for analyzing the rheology of propellants because other type of spindles does not give accurate results due to shear thinning effect observed around the spindle. This viscometer can be operated with eight different rotational speeds of

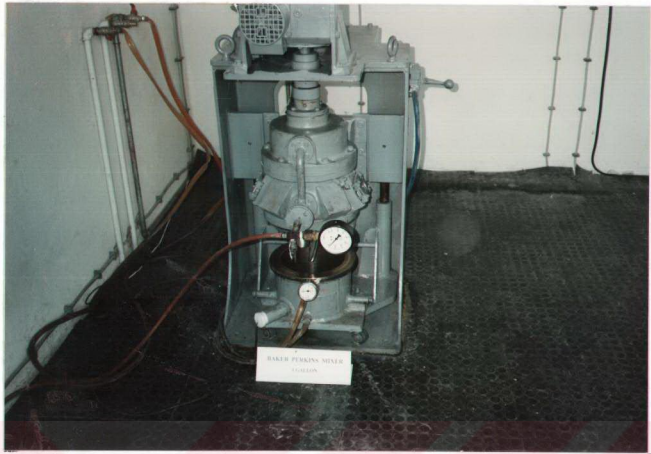


Figure 4.1. Photograph of the 1 gallon Beaker Perkins mixer



Figure 4.2. Photograph of the Brookfield viscometer

0.5, 1, 2.5, 5, 10, 20, 50, and 100 rpm. For this type of viscometers, the recommended sample container is a 600 ml low form Griffin beaker. A constant temperature water bath is installed to maintain the desired temperature. A photograph of the experimental set-up is given in Figure 4.2. Brookfield Viscometers are produced to be accurate to within $\pm 1\%$ of the full-scale range of the spindle/speed combination in use. Reproducibility is within $\pm 0.2\%$. The full-scale range of viscosity for T-A spindle is 16000, 6400, 3200, and 1600 Poise at rotational speeds of 1, 2.5, 5, and 10 rpm, respectively.

For measuring the viscosity, a 500 ml sample of uncured propellant slurry at 65 °C is transferred into the beaker and put in the water bath which is at 65 °C. The spindle which is previously conditioned at 65 °C is attached to the lower shaft of the viscometer while it is in the propellant slurry. The spindle should be centered in the test fluid and immersed to a marked level of the T spindle (T spindles do not have definite immersion levels marked by producer). The rotational speed is adjusted to the slowest value of 0.5 rpm. Then power is turned on and by pressing auto zero button any value kept in the memory is canceled. Spindle code is entered as 91 for T-A spindle. These steps are finished within 5 minutes after the sample propellant is taken from the mixer. Five more minutes are allowed for the propellant slurry to reach steady state that is disturbed earlier during the spindle attachment. This ten minute time period, after taking the sample, should be the same for all the samples to make a reasonable comparison of the viscosities. When all the conditions are satisfied the motor is turned on and the slurry viscosity is displayed on the digital screen. Viscosity value first increases up to a maximum value and then starts to decrease. When the highest value appears the timer is started and readings are

recorded every ten seconds until the time necessary for four revolutions is elapsed. This time is 480 seconds for 0.5 rpm. Then the rotation speed is increased to the next value which is 1 rpm. Again an increase in viscosity is observed up to a certain value. At this value the timer is started and the viscosity is recorded every ten seconds until the time necessary for four revolutions is elapsed. The same procedure is repeated for the six remaining successive rotational speeds, and the viscosities are recorded.

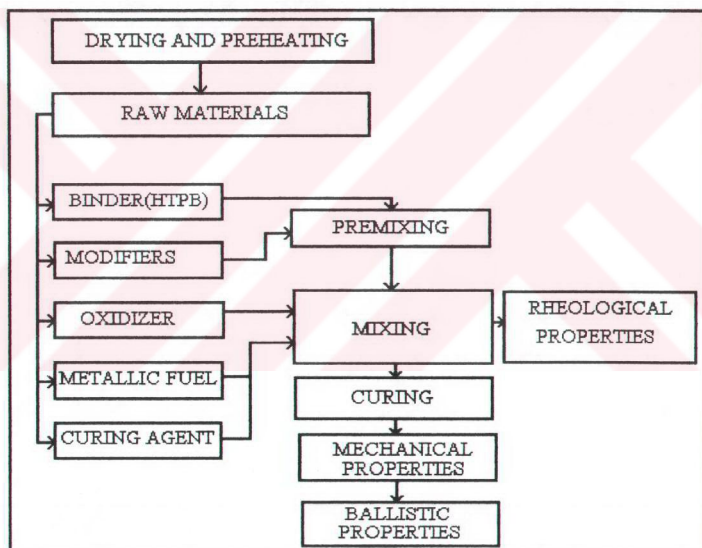


Figure 4.3. Flowchart of the propellant manufacturing process

CHAPTER 5

RESULTS AND DISCUSSIONS

5.1. Application of the Developed Model

The model requires the availability of size distribution of particles used and void fractions of each solid component size. It is therefore necessary to obtain these properties of solids for the application of the model.

5.1.1. Particle size distribution of solid components

The size distributions of the solid components are given in Appendix-A. The results show the frequency of the distribution of sizes based on volume. Obviously, all the components have lognormal particle size distribution. The size distribution of 323.46 μ particles is interrupted at 600 μ and all the particles having diameters greater than this are lumped into 600 μ diameter particles. This is due to the measuring range of the 300 mm lens of the instrument.

The most important parameter to be controlled during the measurements is obscuration. Obscuration is simply the fraction of light 'lost' from the main beam when the sample is introduced. The ideal range for obscuration is between 10% and 30%. The range between 5% and 50% is also usable but results are not as accurate as in the ideal range.

5.1.2. Calculation of void fractions

Determination of void fractions of each component is very critical because the optimum size distribution is highly affected by the average void fractions of component sizes (See Equation 3.1). Calculation of void fractions is based on the measured apparent volumes of the component sizes. There are several methods for void fraction determination, pouring, tapping, and centrifugation. Method of pouring is mostly employed in the storage applications where compression of the particulate is undesired. This method could not be used here because it leaves the highest void volume as compared to the other methods. As its name implies, void fraction is determined by pouring the particles in a container and measuring the apparent volume. Other two methods can be employed for this application, since they both leave relatively small void volumes. In the previous studies, method of mechanical tapping was very often used. In this method, particles are poured into a container by vibration and the container is tapped at definite time intervals. Method of centrifugation was employed in this work mainly due to its ease of application and repeatable results. To test the repeatability of the method, four measurements were

Table 5.1. Void fractions of component sizes

Average Diameter (μ)	Run No	Weight (gr)	Vol. (cm^3)	Apparent density (gr/cm^3)	Particle density (gr/cm^3)	Void fraction	Average void fraction	Standard deviation of void fractions
323.46	1	20	15.8	1.266	1.95	0.3509	0.3742	0.01896
	2	20	16.5	1.212	1.95	0.3784		
	3	20	16.3	1.227	1.95	0.3708		
	4	20	17.0	1.176	1.95	0.3967		
171.12	1	20	17.3	1.156	1.95	0.4071	0.4088	0.00440
	2	20	17.5	1.143	1.95	0.4139		
	3	20	17.4	1.149	1.95	0.4106		
	4	20	17.2	1.163	1.95	0.4037		
31.43	1	20	17.8	1.124	1.95	0.4238	0.4172	0.00467
	2	20	17.5	1.143	1.95	0.4139		
	3	20	17.5	1.143	1.95	0.4139		
	4	20	17.6	1.136	1.95	0.4172		
10.4 (Al)	1	20	13.9	1.439	2.7	0.4671	0.4382	0.02131
	2	20	13.2	1.515	2.7	0.4388		
	3	20	12.7	1.575	2.7	0.4167		
	4	20	13.0	1.538	2.7	0.4302		
9.22	1	20	24.4	0.820	1.95	0.5797	0.5868	0.00667
	2	20	25.0	0.800	1.95	0.5897		
	3	20	24.6	0.813	1.95	0.5831		
	4	20	25.3	0.791	1.95	0.5946		

taken for each component size. Standard deviation of the results of the measurements were calculated and given in Table 5.1.

Once apparent volume is measured, the apparent density can be calculated by dividing the mass of the sample by its apparent volume. Void fraction can then be determined by,

$$\text{Void fraction} = 1 - \frac{\rho_{app}}{\rho_p} \quad (5.1)$$

where ρ_{app} and ρ_p are apparent and particle densities, respectively.

Results of void fractions for all component sizes are given in Table 5.1. Experimental measurements showed that, void fraction of a bed of sizes decreases with increasing average particle diameter. This relation is more obvious in Figure 5.1.

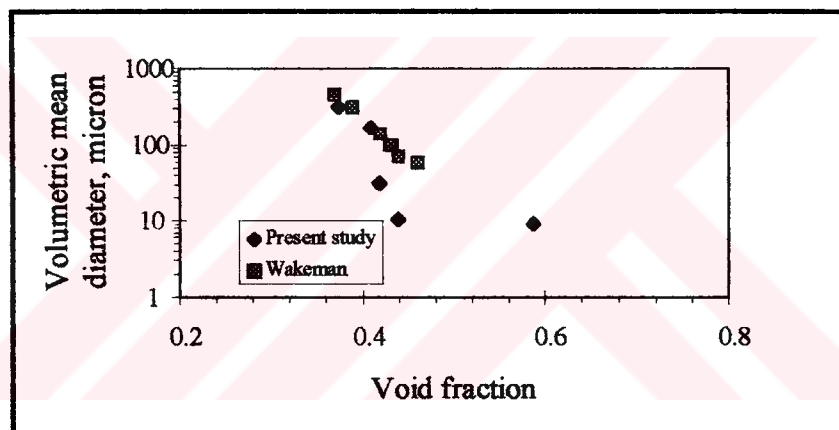


Figure 5.1. Variation of void fraction with mean particle diameter

The increase in void fraction with decreasing particle diameter may be attributed to the particulate interactions. Static electrical forces, friction, adhesion, and other surface forces become increasingly important as particle size decreases, and surface area to volume ratio is markedly increased. Wakeman (1975) observed a semilogarithmic increase in void fraction with decreasing mean particle diameter. A

similar behavior was obtained for ammonium perchlorate particles. If the linear trend of Wakeman's data is extended to the smaller particle diameters, 9.22 μ particles were observed to agree with this linearity. 31.4 μ particles showed a little deviation from this linearity. For Al (10.4 μ) particles, however, a considerable deviation was observed. The Al particles left smaller void fraction than that would be expected for 10.4 μ AP particles. This is mainly because of the particulate characteristics. Al particles have spherical shape which facilitates their dry packing. Here, the Wakeman's data do not have to be in agreement with the data obtained in the present study and it was used only as a reference to see the relation between particle diameter and void fraction.

5.1.3 Calculation of the fractions of the solid component sizes

It was previously mentioned that the size distribution closest to the optimum distribution could be obtained if the proper fractions of the solid components were determined by some means. If this idea is applicable in practice Equation (3.3) should hold. To check whether this equation holds or not, arbitrary values of x_n 's are selected and the distribution of the mixture is determined for each screen size by the use of Equation (3.3). Then a real mixture is prepared with the selected proportions of solid components and its particle size distribution is measured. Using such an approach, aluminum particles (14.12%) and ammonium perchlorate particles (10% of 31.4 μ , 75.88% of 171 μ) were combined and size distribution of the mixture was measured. Figure 5.2 shows the two distributions obtained by

calculation and measuring. As seen from this figure, the distribution obtained by calculation is quite close to that obtained experimentally. Therefore, Equation (3.3) can be used for the determination of optimum size distribution.

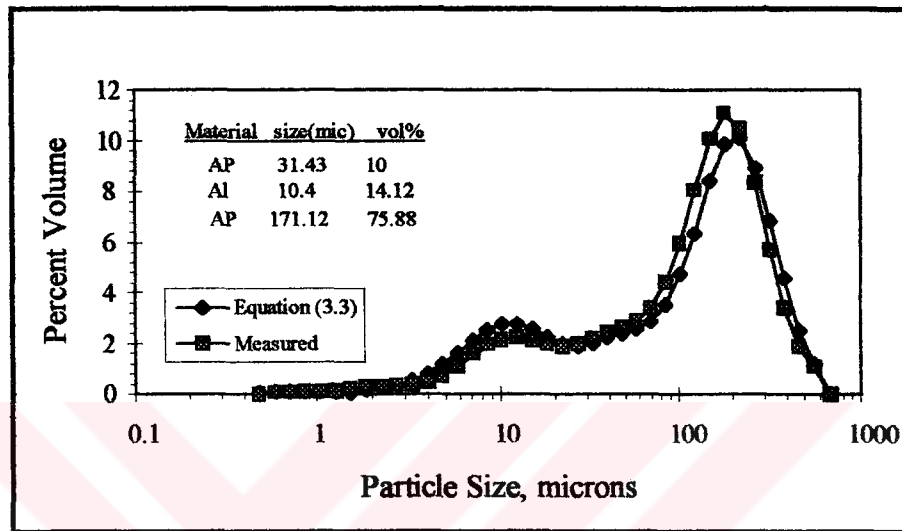


Figure 5.2. Experimental verification of Equation (3.3)

Using the void fractions of solid components from Table 5.1, the optimum size distribution can be obtained by following the procedure given in Section 3.1.1. The smallest screen size is 0.48μ and the succeeding screens have the sizes 1.21 times that of the preceding screen size. The largest screen size is 683μ and the total number of screens is 39. The number of the solid component sizes for all mixtures is 3. A sample for the preparation of optimum size distribution for the set of Al, 9.22μ and 171.12μ ammonium perchlorate particles is given in Table 5.2. The direct results of the optimum size distributions for the other sets are also given in the same

table. Distributions are given as cumulative percent undersize, because the optimum size distribution obtained by Furnas is applicable for this type of distribution. The packing densities of the mixtures are maximum when they have the distributions given in Table 5.2.

The model size distribution was calculated by the use of Equation (3.3). For the model size distribution to be closest to the optimum size distribution, deviation between the two distributions should be minimum. This concept is expressed by Equation (3.4). When this equation is differentiated with respect to x_i 's, the fractions of the solid component sizes can be determined.

Equation (3.4) is composed of 39 terms each containing a second order polynomial. This equation was differentiated and solved by using Winmcad Package. Solutions to this equation for different mixtures are given in Table 5.3. The fractions of the solid components obtained by the model were inserted in Equation (3.3) and the resulting size distribution (model distribution) for each set was plotted in the same graph with the corresponding optimum size distribution. The graphs for the each set are given in Appendix-B. The deviation from the optimum size distribution can be easily visualized from these graphs. For set No.1, there exists a gap for the particle diameters between 25μ and 150μ indicating that some particles of sizes in this range should be removed to increase the packing density of the mixture. Similar gaps are also present for the other sets. For set numbers of 2 and 4, some of the particles having sizes between 200μ and 550μ should be taken out of the mixture. While some particles are to be removed from the mixtures of these sets, some sets require the addition of particles in certain range for maximum packing. Set numbers 3 and 6 are the examples for such a case. The least

Table 5.2. Optimum size distributions for the solid mixtures

Size composition								
Al, 9.22, 171				Al, 9.22	Al, 9.22	Al, 31.4	Al, 31.4	Al, 171
diameter	amount	vol.	cumulative	31.4	323	171	323	323
(μ)	(volumetric)	%	distribution	cumulative percent undersize distribution				
0.48	1.00	1.04	1.04	1.15	1.04	0.93	0.89	0.93
0.59	1.04	1.08	2.12	2.37	2.13	1.91	1.82	1.90
0.71	1.09	1.13	3.24	3.66	3.26	2.93	2.80	2.91
0.86	1.13	1.17	4.42	5.02	4.44	4.00	3.82	3.98
1.04	1.18	1.22	5.64	6.46	5.68	5.12	4.90	5.10
1.26	1.23	1.28	6.92	7.99	6.96	6.29	6.03	6.26
1.52	1.29	1.33	8.25	9.60	8.28	7.52	7.21	7.49
1.84	1.34	1.39	9.64	11.3	9.69	8.81	8.45	8.77
2.23	1.34	1.45	11.09	13.1	11.2	10.1	9.76	10.1
2.7	1.46	1.51	12.60	15.0	12.7	11.6	11.1	11.5
3.27	1.52	1.58	14.17	17.0	14.3	13.1	12.6	13.0
3.95	1.59	1.64	15.81	19.2	15.9	14.6	14.1	14.5
4.79	1.66	1.71	17.53	21.4	17.6	16.2	15.7	16.2
5.79	1.73	1.79	19.31	23.8	19.4	17.9	17.3	17.9
7.01	1.80	1.86	21.18	26.3	21.3	19.7	19.1	19.6
8.48	1.88	1.94	23.12	29.0	23.3	21.6	20.9	21.5
10.3	1.96	2.03	25.15	31.8	25.3	23.5	22.8	23.4
12.4	2.04	2.11	27.26	34.8	27.4	25.6	24.8	25.5
15.1	2.13	2.20	29.47	37.9	29.6	27.7	27.0	27.6
18.2	2.22	2.30	31.76	41.3	31.9	30.0	29.2	29.9
22.0	2.32	2.40	34.16	44.8	34.3	32.3	31.5	32.2
26.7	2.42	2.50	36.66	48.6	36.8	34.8	34.0	34.7
32.3	2.52	2.61	39.27	52.5	39.4	37.4	36.5	37.3
39.1	2.62	2.72	41.99	56.7	42.1	40.1	39.2	40.0
47.3	2.74	2.84	44.82	61.1	44.9	42.9	42.0	42.8
57.3	2.86	2.30	47.78	65.8	47.9	45.9	45.0	45.8
69.3	2.98	3.08	50.87	70.7	51.0	49.0	48.1	48.9
83.9	3.11	3.22	54.08	75.9	54.2	52.2	51.4	52.1
101	3.24	3.35	57.44	81.4	57.6	55.6	54.8	55.6
122	3.38	3.50	60.93	87.3	61.1	59.2	58.4	59.1
148	3.52	3.65	64.58	93.5	64.7	62.9	62.2	62.9
180	3.68	3.81	68.39	100	68.5	66.9	66.2	66.8
218	3.83	3.97	72.35	100	72.5	71.0	70.3	70.9
264	4.00	4.14	76.49	100	76.6	75.3	74.7	75.2
319	4.17	4.32	80.81	100	80.9	79.8	79.3	79.7
386	4.35	4.50	85.31	100	85.4	84.5	84.1	84.4
467	4.53	4.69	90.00	100	90.0	89.4	89.1	89.4
565	4.73	4.89	94.89	100	94.9	94.4	94.4	94.6
683	4.93	5.10	100.0	100	100	100	100	100

deviation from the optimum size distribution is observed for set No 5. From the plots of the size distributions for all the mixtures it can be said that among the available sets, set No 5 contains the particles which are most suitable for maximum packing density. The packing densities for the remaining sets can be ordered in decreasing order as: No 3, No 2, No 4, No 1, and No 6. The most deviation is observed for the sets of 1 and 6. For this reason these tests were not prepared for rheological characterization, since they would exhibit high viscosities.

Table 5.3. Model results for the fractions of the solid components

Set No	Volume fractions of sizes				
	9.22 μ	10.4 μ (Al)	31.4 μ	171 μ	323 μ
1	0.01	0.14	0.85	-	-
2	0.22	0.14	-	0.64	-
3	0.32	0.14	-	-	0.54
4		0.14	0.27	0.59	-
5	-	0.14	0.38		0.48
6	-	0.14	-	0.86	0.00

5.2. Results of Rheological Measurements

The propellant slurries which are to be characterized consist of particles with three different sizes (trimodal mixtures). All possible trimodal combinations of the four different size of ammonium perchlorate particles and aluminum particles were prepared. If aluminum particles are present in every mixture, the possible sets are: Al, 9.22 μ , 31.4 μ / Al, 9.22 μ , 171 μ / Al, 9.22 μ , 323 μ / Al, 31.4 μ , 171 μ / Al,

31.4 μ , 323 μ / Al, 171 μ , 323 μ . Among these, two of the sets were not included in the measurements. These are the sets of (Al, 9.22 μ , 31.4 μ) and (Al, 171 μ , 323 μ) particles. The reason for excluding these sets is that the viscosity of a suspension gets higher as the diameter ratio of the small particles to that of the large particles increases. It was also theoretically determined that these sets have lower packing densities as compared to others. It is, therefore, clear that propellants with these sets of particles will have higher viscosities as compared to the propellants with the other sets.

The results of the experimental measurements for 75% total solid loading are given in Appendix C. When the data are observed it is seen that the viscosity of the propellant slurry varies with time for some propellant slurries, indicating their time dependent (thixotropic) behavior. The propellant slurries showing this property are given in Tables C.1(a, c, d, g, h). It is obvious from the results that the propellant slurries having viscosities greater than 1300 Poise show thixotropic behavior. The thixotropic behavior analysis was based on the measurements taken at 0.5 rpm, because more data are available at this rpm value. For other rpm values the change in viscosity with respect to time is not observable due to the lack of data. Figure 5.3 shows the thixotropic behavior of the propellant slurry the results of which are given in Table C.1(a). The decrease in viscosity continues until certain time value and then increases thereafter due to the curing reaction taking place. The effect of curing reaction is also noticeable in the early stages of the curing. The oscillatory behavior of Figure 5.3 may be attributed to the build-up of the network by cure and its destruction by shear. The shear thinning effect is dominant in the time range in which the measurements were taken. Muthiah et al. (1991) observed the same

oscillatory behavior for the time range between 160 and 200 min. but the overall effect was to increase the viscosity with time. The period of the oscillations also increases with the curing reaction or time. In the experiments, the data recording were ceased after four revolutions of the spindle. The number of revolutions was kept constant at all spindle speeds for avoiding additional experimental parameter.

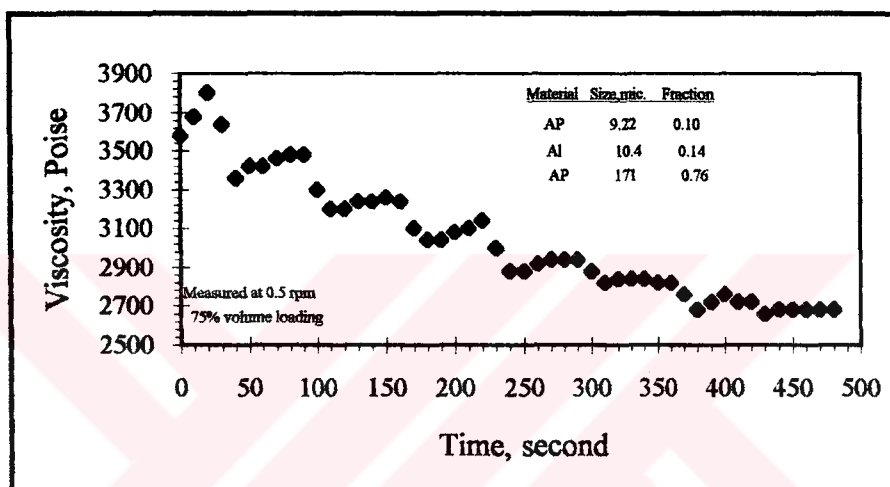


Figure 5.3. Time dependency of the propellant slurry viscosity

The results tabulated in Appendix-C also show the shear rate (rpm) dependency of the uncured propellant slurry viscosity. This indicates the Non-newtonian behavior of the propellants. All the propellants were observed to show Non-newtonian behavior. Figure 5.4 shows the variation in viscosity with respect to the change in the rate of shear. The viscosities plotted on the y axis represent the last reading for each rpm, i.e., reading taken after the four revolutions of the

spindle. The viscosity was observed to increase generally with decreasing rate of shear. This behavior is known as pseudoplastic Non-newtonian behavior.

The results given in Figure 5.4 are in agreement with the results of Osgood (1969). Some results, however, do not show the complete properties of the pseudoplastic behavior. The viscosities given in Tables C.1 (c, f, g, k, o) first decrease then increase with increasing rate of shear showing dilatant flow behavior. These propellants show both pseudoplastic and dilatant flow behavior.

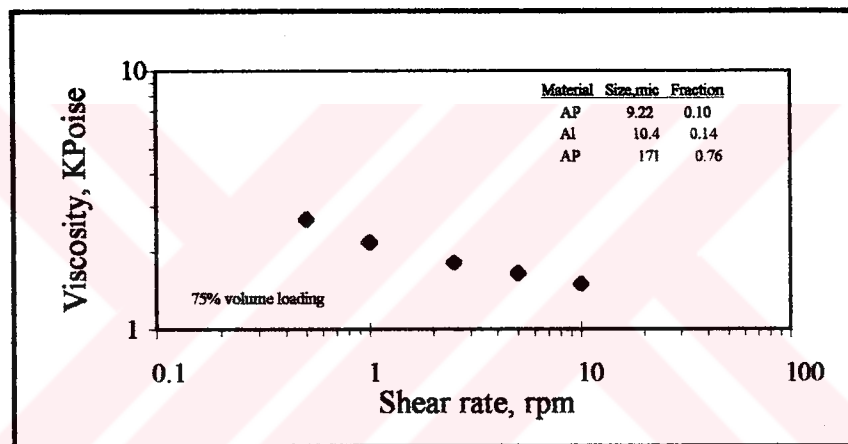


Figure 5.4. Shear rate dependency of the propellant slurry viscosity

The complexity of the flow behavior of the uncured propellant is very obvious from these results. Due to this complexity, it becomes very difficult to make a comparison between the results of different propellants. The time and the rate of shear should be recorded so that a reasonable comparison of viscosities can be made. The Annual Book of ASTM Standards suggests that a constant period of time should elapse before taking a measurement at each rpm or the same number of

revolutions of spindle at each rpm should elapse. In this study, the number of revolutions elapsed was kept constant and measurements were taken after the four revolution of the spindle. The last readings given in Appendix-C are taken as the viscosity data at each speed for all propellants and the results are tabulated in Table 5.4. Among the results given in this table, those which are recorded at 2.5 rpm were used to compare the viscosities. It is known that best characterization of flow behavior is made with results obtained at low shear rates. Another restriction here is that the applied percent torque (unit for torque is dyne-cm) which is proportional to the applied shear stress should be around 10% for the Brookfield Viscometers to be used efficiently. Approximately 10% torque was observed at the 2.5 rpm for all propellants (see Table 5.4) and this rpm value was used for comparison.

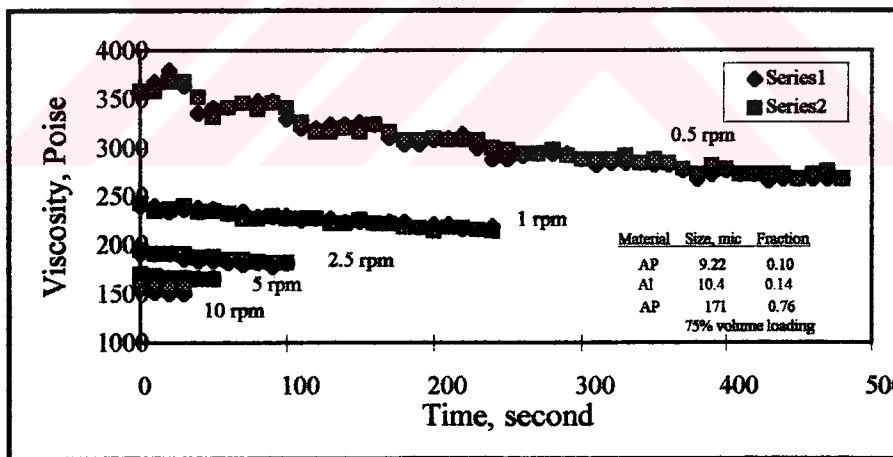


Figure 5.5. The reproducibility of the viscosity measurements

The reproducibility of the Brookfield Viscometer is given within $\pm 0.2\%$.

This is an acceptable limit for comparison. The reproducibility of the measurements

was tested for the propellant the composition of which is the same as that given in Table C.1 (a). The measurements were taken at 65 °C and results are given in Figure 5.5. More tests could be made to obtain the percent experimental reproducibility but these two tests were decided to be sufficient since the results were very close to each other.

5.2.1. Effect of temperature

The most important parameter to be controlled in the measurement of rheological properties is the temperature because the resistance of materials to flow is strongly affected by temperature. Temperature control in the present study is accurate within $\pm 1^\circ\text{C}$. For some systems, even this range is not acceptable as the samples may show very large differences in viscosity with a 0.1°C change in temperature (as stated in the manual of Brookfield Viscometer). It is, therefore, necessary to examine the effect of temperature on the uncured propellant rheology before starting the rheological characterization.

Figure 5.6 shows the change in the viscosity of the uncured propellant slurry with a variation in temperature. The propellant slurry is composed of 10.4μ aluminum particles and 9.22μ and 171μ AP particles and the size ratio of AP particles is 0.132 (fine to coarse). The inverse of absolute temperature (degree K) was used to compare with the results of Muthiah et al. (1991). They used $40\text{--}45\mu$

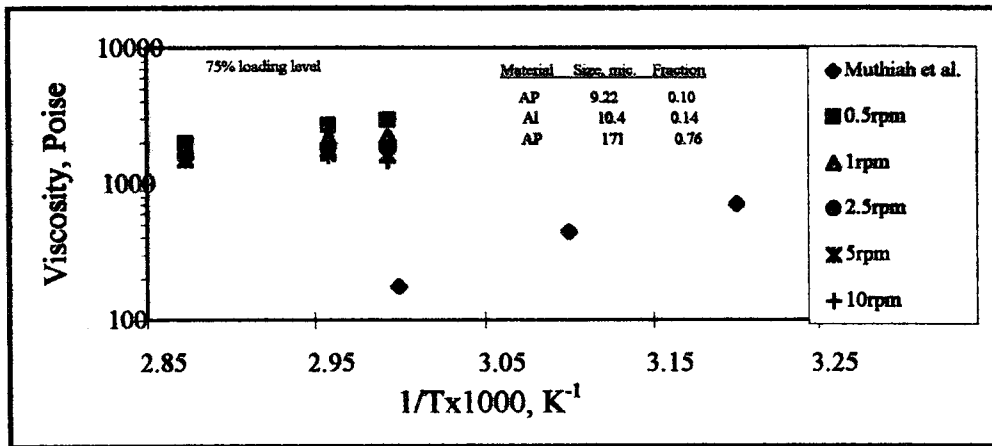


Figure 5.6. Effect of temperature on the viscosity of the uncured propellant

AP particles as fines and 300-325 μ as the coarse fraction with a size ratio of 0.25 (fine to coarse). As expected, viscosity of the uncured propellant increases with decreasing temperature. Muthiah et al. observed a linear relation between the viscosity and the temperature when viscosity is plotted on a logarithmic scale. At high shear rates the relation between viscosity and (1/T) deviates from linearity. Muthiah et al. also observed this behavior. They measured different viscosities from the ones measured in this work. The reason for this is that the particles they used have different diameter ratio and size composition. Also the rate of shear is probably different although it is not reported.

5.2.2. Effect of the mean diameter ratio of the solid components

Two propellant slurries of different mean diameter ratio of solid components were selected to analyze the effect of mean size ratio on the viscosity. One

propellant slurry is composed of 31.4 μ and 171 μ AP particles and the other is composed of 31.4 μ and 323 μ AP particles. The aluminum particles present in both slurries are 10.4 μ in diameter and their content is the same (14.12%) in both. The diameter ratio of the AP components is constant at 0.0972 and 0.1837. The volume fraction of the fine (31.4 μ) AP with respect to the total solid content was varied as 0.27, 0.4, and 0.55.

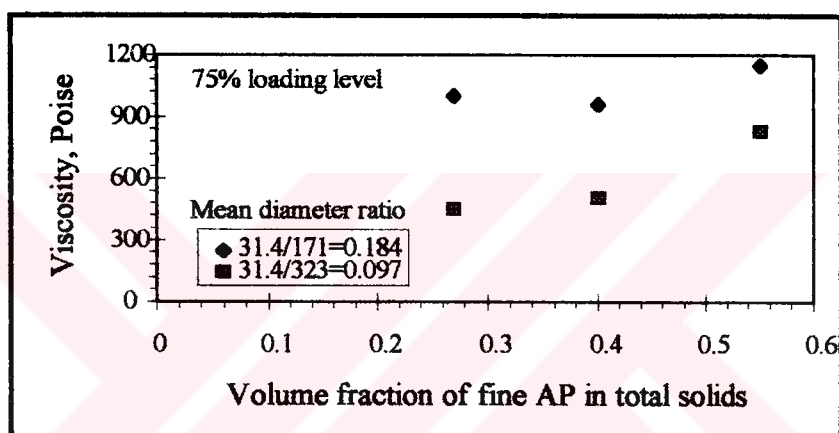


Figure 5.7. Effect of mean diameter ratio on the viscosity (at 2.5 rpm) of the uncured propellant

The change in viscosity with respect to the mean diameter ratio of the solid components is given in Figure 5.7. The measurements show that viscosity of both propellants decreases with decreasing mean diameter ratio of the components. The observation was made considering the AP particles only. However, the consideration of aluminum particles as well, does not yield different results as the mean diameter of aluminum particles is smaller than both AP's. The effect of mean

Table 5.4. The results of the viscosity measurements of the propellant slurries at different rpm's

Set No	Size composition	Volume fraction of fine AP	Viscosity (Poise)									
			0.5rpm Torque	1rpm Torque	2.5rpm Torque	5rpm Torque	10rpm Torque	15rpm Torque	20rpm Torque	25rpm Torque	30rpm Torque	35rpm Torque
2	Al	0.10	2680	8.4	2160	23.4	1810	28	1660	51.5	1590	97.7
	9.22 μ	0.24	864	2.7	800	5	776	12	768	24.1	784	48.8
	171 μ	0.40	1380	4.3	1260	7.8	1230	19.2	1290	40.2	1410	87.8
3	Al	0.04	1250	3.7	1010	6.2	824	12.9	720	22.6	685	41.5
	9.22 μ	0.15	704	2.1	640	3.9	564	8.9	540	17.1	523	32.8
	323 μ	0.33	704	2.1	656	4.1	648	10	668	20.9	694	43.4
4	Al	0.50	1470	4.5	1380	8.6	1350	21.1	1430	44.5	1540	96.2
	31.4 μ	0.10	3520	9.7	2590	16.5	1760	26.6	1260	36.3	832	48.8
	171 μ	0.27	1180	3.7	1090	6.8	1000	15.6	966	30.2	928	58.2
5	Al	0.40	1060	3.3	992	6.2	960	15	950	29.7	936	58.8
	31.4 μ	0.52	1220	3.8	1170		1150	18	1160	36.4	1170	73
	323 μ	0.15	608	1.9	512	3.3	472	7.4	448	14.2	429	27.1
5	31.4 μ	0.30	544	1.7	480	3	448	7	442	13.9	438	27.2
	323 μ	0.55	832	2.6	816	5.1	824	13	832	26.1	848	53.3
		0.40	544		528		504		506		507	

diameter ratio can also be observed for other propellant slurries from Table 5.4. For the propellants containing 9.22 μ particles, the expected trend is not observed. When the propellants with (Al, 9.22 μ , 171 μ) and (Al, 31.4 μ , 171 μ) solids are compared, it is seen that the propellant with smaller diameter ratio (small to large) has greater viscosity. This can be explained by the closeness of the mean diameter of aluminum particles to 9.22 μ . The 31.4 μ particles are used to fill the voids that remain after the combination of the Al and coarse AP. It is very obvious that when three solid components are mixed for maximum packing (or for minimum viscosity), the medium size component should be close to the average of the fine and coarse components. This is valid of course if the range of size, shape of particles, density of particles etc. are the same for all the components.

5.2.3. Effect of fractional variations of components

The change in the viscosity of a slurry with respect to the changes in the fractions of the components in the total solids is better understood by using the concept of packing fraction. For this, the relation derived by Maron and Pierce as given by Gupta (1986) is used.

$$\eta_r = \left(1 - \frac{\phi}{\phi_p}\right)^{-2} \quad (5.2)$$

In Equation 5.2, η_r is the relative viscosity defined as the ratio of the suspension viscosity to the suspending medium viscosity, ϕ is the total volume fraction of solids in the slurry, and ϕ_p is the maximum packing fraction of the system at a specified total solid content. According to this equation, viscosity is a function of the total volume fraction of the solids and the maximum packing fraction at this loading level, i.e., $\eta_r = f(\phi / \phi_p)$. The relative viscosity is expected to decrease with the increasing maximum packing fraction of the system the loading level being constant.

Figure 5.8 shows the effect of compositional variation on the relative viscosity of the propellant slurry. The viscosity of the unfilled polymer matrix at different shear rates are given in Table C.1 (p). The relative viscosities in Figure 5.8 were determined by dividing the viscosity of the slurry by the viscosity of the unfilled polymer matrix measured at 2.5 rpm. It is seen that the relative viscosities of both

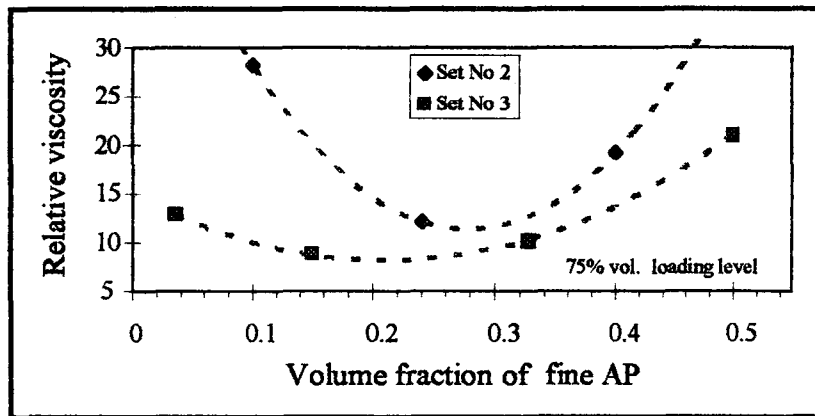


Figure 5.8. Effect of fraction of the fines in the total solids on the viscosity of the propellant slurry (set numbers are given in Table 5.4)

propellant slurries first decrease with increasing concentration of the fines and then increase with further increase in the fines concentration showing minima. A second order polynomial trendline was inserted to determine this minimum viscosity clearly. It can be deduced from the Figure 5.8 that packing fraction (ϕ_p) of the solids mixture increases until the concentration of the fines (9.22 μ) becomes 0.28. The viscosity of the slurry containing these particles decreases because (ϕ/ϕ_p) decreases. At the point where the fraction of the fines is 0.28, the packing fraction of the system reaches its maximum attainable value and (ϕ/ϕ_p) becomes minimum. At this point ϕ_p is equal to ϕ_{max} . After this point, ϕ_p begins to decrease with further increase in fines fraction. The relative viscosity at maximum packing condition is equal to 12 in set number 2.

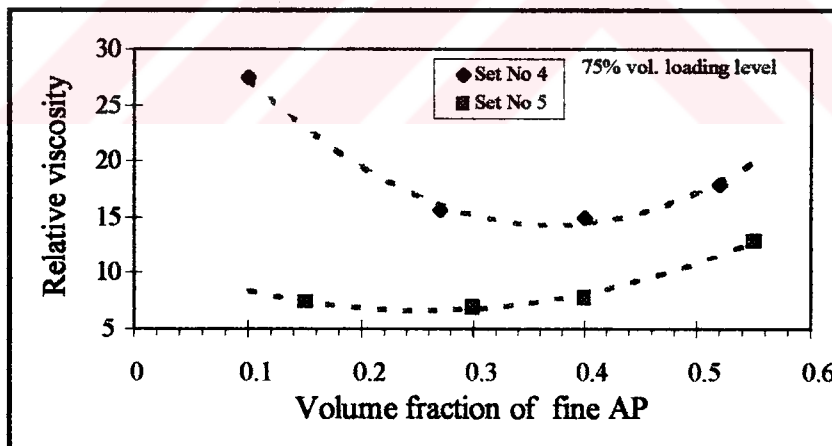


Figure 5.9. Effect of fraction of the fines in the total solids on the viscosity of the propellant slurry (set numbers are given in Table 5.4)

At maximum packing condition, the fractions of the solid components and the corresponding minimum viscosities can be determined for the other propellant slurries similarly. For the other propellants, the variation in the viscosity with respect to the concentration of fine AP is given in Figures 5.8 and 5.9. The minimum relative viscosities for the propellants for sets No 3, No 4, and No 5 are 8.8, 15, and 7, respectively. All of these are the minimum viscosities of each set. Among these, the propellant with minimum viscosity, that is, the minimum of the minimums is selected as the most processable one. The propellant consisting of 31.4 μ and 323 μ AP particles and 10.4 μ aluminum particles was found to have maximum fluidity (minimum viscosity) at the fines fraction of 0.3. It was decided to be used as the candidate propellant for increasing the solid loading which is discussed in the next section.

5.2.4. Effect of solid loading

In the previous section, the system having maximum packing fraction was determined by keeping the solid loading level constant. Here the total volume concentration of the propellant will be increased at the determined maximum packing fraction. In this analysis Equation 5.2 was modified as:

$$\eta_r = \left(1 - \frac{\phi}{\phi_m}\right)^{-2} \quad (5.3)$$

The relative viscosity now becomes a function only of the solid loading and maximum packing fraction, that is, $\eta_r = f(\phi / \phi_m)$.

The change in the relative viscosity with increasing loading level is given in Figure 5.10. The lower limit for total volume concentration of the solids was selected to be 0.75, since the propellant with this loading level is already being processed. The relative viscosity of the propellant slurry was observed to increase as expected from Equation 5.3. This increase is caused by the increase in (ϕ / ϕ_m) ratio. This ratio approaches unity when the total volume concentration of the solids gets closer to the maximum packing fraction of the system. At this condition the relative viscosity of the system becomes infinity showing an asymptotic behavior.

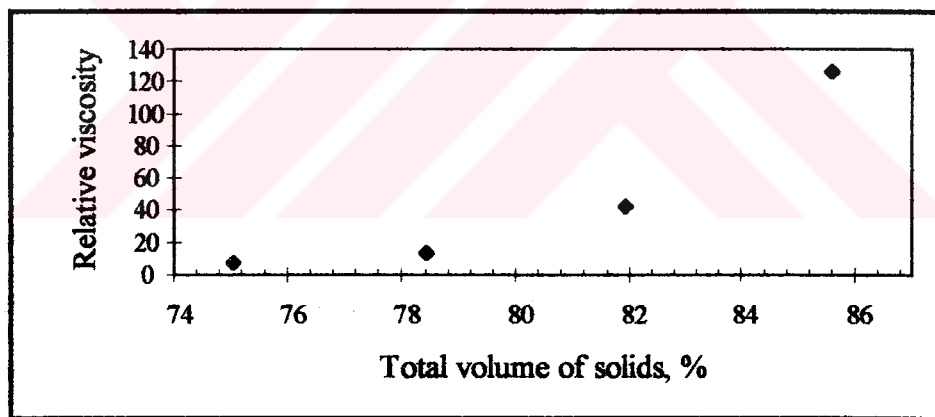


Figure 5.10. Variation in viscosity of the propellant with increasing total volume concentration of solids

5.3. Comparison of Model and Experimental Results

Volume fractions of the solid components, for maximum packing, determined by modeling and by viscosity measurements (experimental) are given in Table 5.5. The last column shows the deviation of the model from the experimental values. The deviation was calculated with respect to the fractions of the coarse AP particles of the minimum viscosity propellant, considering that the experimental results are correct. A maximum of 18% deviation from the experimental results was observed. Although this is acceptable in engineering applications, the reasons should be clarified from a scientific point of view.

The solid particles used in propellant manufacturing have irregular shapes except for the aluminum powder. However, Furnas' method that gives the optimum particle size distribution was developed for spherical particles. This can be considered as one of the possible reasons.

Table 5.5. Comparison of the model results with the experimental findings

Set No	Volume fractions of sizes										Percent deviation of model
	9.22 μ		10.4 μ		31.4 μ		171 μ		323 μ		
	Model	Exp	Model	Exp	Model	Exp	Model	Exp	Model	Exp	
2	0.22	0.28	0.14	0.14	-	-	0.64	0.58	-	-	10
3	0.32	0.2	0.14	0.14	-	-	-	-	0.54	0.66	18
4	-	-	0.14	0.14	0.27	0.36	0.59	0.50	-	-	18
5	-	-	0.14	0.14	0.38	0.30	-	-	0.48	0.56	14

The void fractions which are the inputs for the optimum size distribution were determined by dry mixing of the particulates. Dry mixing may yield inaccurate void fraction measurements, since the solid particles can not be perfectly mixed in dry conditions. The particles were also mixed in a liquid (n-Heptane) in which the particles are insoluble, but this method gave higher void fraction than that obtained by dry mixing due to bridging that formed during the drying of n-Heptane. High void fraction means low packing fraction. The aim of this study is to obtain maximum packing fraction of the particulate, therefore this method was not used for the determination of void fractions.

Furnas' method is known to give the optimum size distribution if the number of component sizes are determined theoretically as described by Furnas (1931). This is a trial-and-error procedure and the number of component sizes is a function of the void fraction of the components and the diameter ratio of the smallest size to the largest one. When this theoretical approach was made, the number of component sizes was found to be two. However, it is known that the packing fraction of the particulate system increases with increasing number of solid components. Due to this fact, the model was modified for three component sizes. This probably caused the developed model to deviate from the optimum size distribution.

Similar studies for maximum packing were performed using particles with very large diameters as compared to the particles used in this study. Furnas' method was tested only for the particles with large diameters (in the order millimeters), such as sand, aggregates, etc. On the other hand, the maximum particle diameter in this study is only 600 μ . Although no restriction was given by Furnas in terms of particle diameter, the deviation of the model may also be due to this reason.

The diameter ratio (large to small) of the two consecutive sizes for the optimum distribution was taken as 1.41 by Furnas. In this study, it was taken as 1.21. Using this ratio simplifies the calculations because the particle diameter measuring instrument gives the distribution according to this ratio. Different values of this ratio could be tested to see its effect on the deviation of the model. This requires a parametric study and is out of the scope of this study.



CHAPTER 6

CONCLUSIONS AND RECOMMENDATIONS

The developed method of centrifugation is a good method for the determination of void fraction, because it yields repeatable results. The standard deviations of the measurements obtained by this method are given in Table 5.1.

The HTPB based uncured propellants showed time dependent (thixotropic) behavior especially when they have viscosities greater than 1300 P, measured at 0.5 rpm with T-A spindle. For viscosities below 1300 P, no time dependency was observed. The time dependency of the uncured propellants showed an oscillatory behavior due to the presence of the curing reaction. The propellant slurry showed thixotropic behavior when shearing is dominant. However, when the curing reaction dominates which is the case after the two hours of curing, viscosity of the propellants increased with time (rheopectic behavior). The propellant slurry also showed pseudoplastic (shear rate thinning) behavior (See Figure 5.4).

The logarithm of the viscosity of the propellant slurry increased linearly with $(1/T)$. The viscosity also decreased with decreasing mean size ratio (small to large).

Among the four candidate propellants, the one consisting of particles with mean diameters of 10.4μ , 31.4μ and 323μ was found to yield minimum viscosity.

This minimum viscosity was observed when the fraction of the sizes with respect to total solids is 0.1412, 0.3 and 0.5588 respectively.

The viscosity of the uncured propellant increased with increasing total solid content showing an asymptotic behavior. The propellant was found to be processable at 82 % volume loading level with a slurry viscosity of 2730 Poise at 2.5 rpm.

The results obtained by the model showed a maximum of 18% deviation calculated with respect to the fraction of the coarse AP of the minimum viscosity propellant. This deviation is acceptable in engineering applications.

For future work, it is recommended that the validity of the developed model be checked by applying it to mixtures of higher modalities and comparing the results with the viscosity measurements on corresponding propellant slurries.

REFERENCES

Anderegg, F.O., 1931, "Grading Aggregates II-The Application of Mathematical Formulas to Mortars" *Ind. Eng. Chem.*, 23, 1058

Chen, J.K., Hsu, J.S., 1986, "An Empirical Model for Prediction of the Slurry Viscosity of AP/HTPB Propellant" *17th International Conference of ICT*, Ch. 38, 1

Chong, J.S., Christiansen, E.B., Baer, A.D., 1971, "Rheology of Concentrated Suspensions" *Journal of Applied Polymer and Science*, 15, 2007

Farris, R.J., 1968, "Prediction of the Viscosity of Multimodal Suspensions from Unimodal Viscosity Data" *Transactions of the Society of Rheology*, 12(2), 281

Fidleris, V., Whitmore, R.N., 1961, *Rheol. Acta*, 1(4-6), cited in Farris (1968)

Fuller, W.B., Thompson, S.E., 1907, *Trans. Am. Soc. Civ. Eng.*, 59, 67, cited in Yu and Standish (1992)

Furnas, C.C., 1931, "Grading Aggregates I-Mathematical Relations for Beds of Broken Solids of Maximum Density" *Industrial and Engineering Chemistry*, 23, 1052

Gray, W.A., 1968, in "The Packing of Solid Particles" Chapman and Hall Ltd, London, Ed. Williams, J.C.

Gupta, R.K., Seshadri, S.G., 1986, "Maximum Loading Levels in Filled Liquid Systems" *Journal of Rheology*, 30(3), 503

Hadhoud, M.K., Haleim, O.A., Sadek, M.A., Abdel Wahab, M.A., 1982, "Rheological and Explosive Properties of Plastic Bonded High Explosives Based on HTPB" *Intern Jahrestag Fraunhofer Inst Treib Explosivstoffe*, 25, 277

Haughey, D.P., Beveridge, G.S.G., 1969, "Structural Properties of Packed Beds-A review" *The Canadian Journal of Chemical Engineering*, 47, 130

- Hoffman, R.L., 1992, "Factors Affecting the Viscosity of Unimodal and Multimodal Colloidal Dispersions" *Journal of Rheology*, 36(5), 947
- Kamal, M.R., Mutel, A., 1985, "Rheological Properties of Suspensions in Newtonian and Non-Newtonian Fluids" *Journal of Polymer Engineering*, 5(4), 293
- Kataoka, T., Kitano, T., Nishimura, T., 1978, "Utility of Parallel-Plate Plastometer for Rheological Study of Filled Polymer Melts" *Rheol. Acta*, 17(6), 626
- Ke-Xi, Y., Ze-Ming, T., Guo-Juan, W., 1986, "Viscosity Prediction of Composite Solid Propellant Slurry" *Propellants, Explosives, Pyrotechnics*, 11, 167
- Kishore, K., Sunitha, M.R., "Effect of Transition Metal Oxides on Decomposition and Deflagration of Composite Solid Propellant Systems: A Survey" *AIAA Journal*, 17(10), 1118
- Klager, K. et al., 1978, "Rheology of Composite Solid Propellant During Motor Casting" *Internationale Jahrestagung ICT*, 141
- Kubota, N., 1984, *Fundamentals of Solid-Propellant Combustion*, Edited by Kuo K.K., Summerfield, M., Progress in Astronautics and Aeronautics, vol. 90, 1
- Landel, R.F., Moser, B.G., Bauman, A.J., 1965, "Rheology of Concentrated Suspensions: Effect of a Surfactant" *Proceedings of the Fourth International Congress on Rheology*, New York, Part 2, 663
- Manual of Brookfield Viscometer, Manual No. M/92-161-E593
- Maron, S.H., Madow, B.P., Krieger, I.M., 1951, "Rheology of Synthetic Latex II. Concentration Dependence of Flow in Type V GR-S Latex" *J. Colloid. Sci.*, 6, 584
- McGeary, R.K., 1961, "Mechanical Packing of Spherical Particles" *Journal of the American Ceramic Society*, 44(10), 513
- Messing, C.L., Onada, G.Y., 1978, "Inhomogeneity- Packing Density relations in Binary Powders-Experimental Studies" *Journal of the American Ceramic Society*, 61(7-8), 363
- Messing, C.L., Onada, G.Y., 1978, "Inhomogeneity- Packing Density relations in Binary Powders" *Journal of the American Ceramic Society*, 61(1-2), 1

Metzner, A.B., 1985, "Rheology of Suspensions in Polymeric Liquids" *Journal of Rheology*, 29(6), 739

Mewis, J., Bleyser, R., 1975, "Concentration Effects in Viscoelastic Dispersions" *Rheol. Acta*, 14(8), 721

Milewski, J.V., 1978, "The Combined Packing of Rods and Spheres in Reinforcing Plastics" *Ind. Eng. Chem. Prod. Res. Dev.*, 17(4), 363

Miller, R.R., Lee E., Powell R.L., 1991, "Rheology of Solid Propellant Dispersions" *Journal of Rheology*, 35(5), 901

Muthiah, R.M., Krishnamurthy, V.N., and Gupta, B.R., 1992, "Rheology of HTPB Propellant. I. Effect of Solid Loading, Oxidizer Particle Size and Aluminum Content" *J. Applied Polymer Science*, 44, 2043

Muthiah, R.M., Manjari R., Krishnamurthy, V.N., Gupta, B.R., 1991, "Effect of Temperature on the Rheological Behaviour of HTPB Propellant Slurry" *Polymer Engineering and Science*, 31(2), 61

Osgood, A.A., 1969, "Rheological Characterization of Non-Newtonian Propellants for Casting Optimization" *AIAA* paper no 69-518, 1

Ouchiyama, N., Tanaka, T., 1980, "Estimation of the Average Number of Contacts between Randomly Mixed Solid Particles" *Ind. Eng. Chem. Fund.*, 19, 338

Ouchiyama, N., Tanaka, T., 1981, "Porosity of a Mass of Solid Particles Having a Range of Sizes" *Ind. Eng. Chem. Fund.*, 20, 66

Ouchiyama, N., Tanaka, T., 1984, "Porosity Estimation for Random Packings of Spherical Particles" *Ind. Eng. Chem. Fundam.*, 23, 490

Poslinski, A.J., Ryan, M.E., Gupta, R.K., Seshadri, S.G., Frechette, F.J., 1988, "Rheological Behaviour of Filled Polymeric Systems II- The Effect of a bimodal Size Distribution of Particulates" *Journal of Rheology*, 32(8), 751

Povinalli, L.A., Rosenstein, R.A., 1964, "Alumina Size Distributions from High-Pressure Composite Solid-Propellant Combustion" *AIAA Journal*, 2(10), 1754

Probstein, R.F., Sengun, M.Z., Tseng, T.C., 1994, "Bimodal Model of Concentrated Suspension Viscosity for Distributed Particle Sizes" *Journal of Rheology*, 38(4), 811

Reji, J., Ravindran, P., Neelakantan, N.R., Subramanian, N., 1991, "Viscometry of Isothermal Urethane Polymerization" *The Chemical Society Japan Bulletin*, 64, 3153

Roscoe, R., 1952, *Brit. J. Appl. Phys.*, 3, 267, cited in Sweeney and Geckler(1954)

Russel, W.B., 1980, "Review of the Role of Colloidal Forces in the Rheology of Suspensions" *Journal of Rheology*, 24(3), 287

Shapiro, A.P and Probstein, R.F., 1992, "Random Packing of Spheres and Fluidity Limits of Monodispersed and Bidispersed Suspensions" *Physical Review Letters*, 68(9), 1422

Sohn, H.Y., Moreland, C., 1968, "The Effect of Particle Size Distribution on Packing Density" *The Canadian Journal of Chemical Engineering*, 46, 162

Sweeney, K.H., and Geckler, R.D., 1954, "The Rheology of Suspensions" *Journal of Applied Physics*, 25(9), 1135

Tulis, A.J., 1986, "The Influence of Particle Size on Energetic Formulations" *17th International Annual Conference of ICT*, Ch. 40, 1

Wakeman, R.J., 1975, "Packing Densities of Particles with Log-Normal Size Distributions" *Powder Technology*, 11, 297

Weast, R.C., 1974, "Handbook of Chemistry and Physics" CRC Press, Inc., 55th Edition

Yu, A.B., Standish, N. A., 1993, "Study of the Packing of Particles with a Mixture Size Distribution" *Powder Technology*, 76, 113

Zok, F., Lange, F.F. and Porter, J.R., 1991, "Packing Density of Composite Powder Mixtures" *J. Am. Ceram. Soc.*, 74(8), 1880

APPENDIX A

Table A.1. Size distribution of 9.22 micron AP particles


		TÜRKİYE BİLİMSEL VE TEKNİK ARAŞTIRMA KURUMU SAVUNMA SANAYİİ ARAŞTIRMA VE GELİŞTİRME ENSTİTÜSÜ																																																																																																																																							
Presentation: 2RHA Polydisperse model Sample: AP , 77 Focus = 100 mm.		9 micron AP Run No. 1 Source: Analysed Beam Length = 2.4 mm.																																																																																																																																							
		Volume Result Obscuration = 13.3 %																																																																																																																																							
Measured on: 07 Nov 1994 15:02 Analysed on: 07 Nov 1994 15:02 Last Saved: 07 Nov 1994 15:02 Configuration file: SIZER Sample Path: C:\SIZER\DATA\		Sampler: MSX64																																																																																																																																							
Residual = 0.277 % Uniformity = 0.712 Specific S.A. = 0.8834 sq. m. /gm. d (v, 0.5) = 7.38 um d (v, 0.1) = 1.41 um		Concentration = 0.006 % Span = 1.987 Mode = 8.73 um d (v, 0.9) = 16.07 um																																																																																																																																							
D [4, 3] = 9.22 um		D [3, 2] = 3.48 um.																																																																																																																																							
<table border="1" style="width: 100%; border-collapse: collapse;"> <thead> <tr> <th>Size (Lo) um</th> <th>Volume In %</th> <th>Size (Hi) um</th> <th>Volume Below %</th> </tr> </thead> <tbody> <tr><td>0.20</td><td>0.65</td><td>0.48</td><td>0.65</td></tr> <tr><td>0.48</td><td>1.71</td><td>0.59</td><td>2.36</td></tr> <tr><td>0.59</td><td>2.25</td><td>0.71</td><td>4.61</td></tr> <tr><td>0.71</td><td>2.16</td><td>0.86</td><td>6.76</td></tr> <tr><td>0.86</td><td>1.64</td><td>1.04</td><td>8.41</td></tr> <tr><td>1.04</td><td>1.10</td><td>1.26</td><td>9.50</td></tr> <tr><td>1.26</td><td>0.83</td><td>1.52</td><td>10.33</td></tr> <tr><td>1.52</td><td>0.96</td><td>1.84</td><td>11.29</td></tr> <tr><td>1.84</td><td>1.44</td><td>2.23</td><td>12.73</td></tr> <tr><td>2.23</td><td>2.26</td><td>2.70</td><td>14.99</td></tr> <tr><td>2.70</td><td>3.32</td><td>3.27</td><td>18.31</td></tr> <tr><td>3.27</td><td>4.69</td><td>3.95</td><td>23.01</td></tr> <tr><td>3.95</td><td>6.32</td><td>4.79</td><td>29.32</td></tr> <tr><td>4.79</td><td>8.09</td><td>5.79</td><td>37.41</td></tr> <tr><td>5.79</td><td>9.74</td><td>7.01</td><td>47.15</td></tr> <tr><td>7.01</td><td>10.90</td><td>8.48</td><td>58.05</td></tr> </tbody> </table>	Size (Lo) um	Volume In %	Size (Hi) um	Volume Below %	0.20	0.65	0.48	0.65	0.48	1.71	0.59	2.36	0.59	2.25	0.71	4.61	0.71	2.16	0.86	6.76	0.86	1.64	1.04	8.41	1.04	1.10	1.26	9.50	1.26	0.83	1.52	10.33	1.52	0.96	1.84	11.29	1.84	1.44	2.23	12.73	2.23	2.26	2.70	14.99	2.70	3.32	3.27	18.31	3.27	4.69	3.95	23.01	3.95	6.32	4.79	29.32	4.79	8.09	5.79	37.41	5.79	9.74	7.01	47.15	7.01	10.90	8.48	58.05	<table border="1" style="width: 100%; border-collapse: collapse;"> <thead> <tr> <th>Size (Lo) um</th> <th>Volume In %</th> <th>Size (Hi) um</th> <th>Volume Below %</th> </tr> </thead> <tbody> <tr><td>8.48</td><td>11.15</td><td>10.27</td><td>69.20</td></tr> <tr><td>10.27</td><td>10.23</td><td>12.43</td><td>79.44</td></tr> <tr><td>12.43</td><td>8.29</td><td>15.05</td><td>87.73</td></tr> <tr><td>15.05</td><td>5.81</td><td>18.21</td><td>93.54</td></tr> <tr><td>18.21</td><td>3.37</td><td>22.04</td><td>96.90</td></tr> <tr><td>22.04</td><td>1.48</td><td>26.68</td><td>98.38</td></tr> <tr><td>26.68</td><td>0.34</td><td>32.29</td><td>98.72</td></tr> <tr><td>32.29</td><td>0.00</td><td>39.08</td><td>98.72</td></tr> <tr><td>39.08</td><td>0.00</td><td>47.30</td><td>98.72</td></tr> <tr><td>47.30</td><td>0.00</td><td>57.25</td><td>98.72</td></tr> <tr><td>57.25</td><td>0.05</td><td>69.30</td><td>98.77</td></tr> <tr><td>69.30</td><td>0.35</td><td>83.87</td><td>99.12</td></tr> <tr><td>83.87</td><td>0.53</td><td>101.52</td><td>99.65</td></tr> <tr><td>101.52</td><td>0.35</td><td>122.87</td><td>100.00</td></tr> <tr><td>122.87</td><td>0.00</td><td>148.72</td><td>100.00</td></tr> <tr><td>148.72</td><td>0.00</td><td>180.00</td><td>100.00</td></tr> </tbody> </table>	Size (Lo) um	Volume In %	Size (Hi) um	Volume Below %	8.48	11.15	10.27	69.20	10.27	10.23	12.43	79.44	12.43	8.29	15.05	87.73	15.05	5.81	18.21	93.54	18.21	3.37	22.04	96.90	22.04	1.48	26.68	98.38	26.68	0.34	32.29	98.72	32.29	0.00	39.08	98.72	39.08	0.00	47.30	98.72	47.30	0.00	57.25	98.72	57.25	0.05	69.30	98.77	69.30	0.35	83.87	99.12	83.87	0.53	101.52	99.65	101.52	0.35	122.87	100.00	122.87	0.00	148.72	100.00	148.72	0.00	180.00	100.00
Size (Lo) um	Volume In %	Size (Hi) um	Volume Below %																																																																																																																																						
0.20	0.65	0.48	0.65																																																																																																																																						
0.48	1.71	0.59	2.36																																																																																																																																						
0.59	2.25	0.71	4.61																																																																																																																																						
0.71	2.16	0.86	6.76																																																																																																																																						
0.86	1.64	1.04	8.41																																																																																																																																						
1.04	1.10	1.26	9.50																																																																																																																																						
1.26	0.83	1.52	10.33																																																																																																																																						
1.52	0.96	1.84	11.29																																																																																																																																						
1.84	1.44	2.23	12.73																																																																																																																																						
2.23	2.26	2.70	14.99																																																																																																																																						
2.70	3.32	3.27	18.31																																																																																																																																						
3.27	4.69	3.95	23.01																																																																																																																																						
3.95	6.32	4.79	29.32																																																																																																																																						
4.79	8.09	5.79	37.41																																																																																																																																						
5.79	9.74	7.01	47.15																																																																																																																																						
7.01	10.90	8.48	58.05																																																																																																																																						
Size (Lo) um	Volume In %	Size (Hi) um	Volume Below %																																																																																																																																						
8.48	11.15	10.27	69.20																																																																																																																																						
10.27	10.23	12.43	79.44																																																																																																																																						
12.43	8.29	15.05	87.73																																																																																																																																						
15.05	5.81	18.21	93.54																																																																																																																																						
18.21	3.37	22.04	96.90																																																																																																																																						
22.04	1.48	26.68	98.38																																																																																																																																						
26.68	0.34	32.29	98.72																																																																																																																																						
32.29	0.00	39.08	98.72																																																																																																																																						
39.08	0.00	47.30	98.72																																																																																																																																						
47.30	0.00	57.25	98.72																																																																																																																																						
57.25	0.05	69.30	98.77																																																																																																																																						
69.30	0.35	83.87	99.12																																																																																																																																						
83.87	0.53	101.52	99.65																																																																																																																																						
101.52	0.35	122.87	100.00																																																																																																																																						
122.87	0.00	148.72	100.00																																																																																																																																						
148.72	0.00	180.00	100.00																																																																																																																																						
Malvern Instruments Ltd. Malvern, U.K.		MasterSizer X Ver. 1.2b Serial No.																																																																																																																																							
		29 Dec 95 09:42																																																																																																																																							

Table A.2. Size distribution of 10.4 micron (Al) particles



**TÜRKİYE BİLİMSEL VE TEKNİK ARAŞTIRMA KURUMU
SAVUNMA SANAYİİ ARAŞTIRMA VE GELİŞTİRME ENSTİTÜSÜ**

Aluminum ALCAN X-65 Run No. 28

Presentation: 2RHA
Polydisperse model
Sample: AP , 171
Focus = 100 mm.

Source: Averaged
Beam Length = 2.4 mm.

Volume Result
Obscuration = 16.8 %

Measured on: 20 Apr 1995 10:36
Analysed on: 20 Apr 1995 11:03
Last Saved: 21 Apr 1995 11:08
Configuration file: SIZER
Sample Path: C:\SIZER\DATA\

Sampler: MSX64

Residual = 0.532 % Concentration = 0.017 %
Uniformity = 0.495 Span = 1.452
Specific S.A. = 0.3101 sq. m. /gm.
d (v, 0.5) = 8.93 µm Mode = 9.30 µm D [4, 3] = 10.40 µm
d (v, 0.1) = 4.34 µm d (v, 0.9) = 17.30 µm D [3, 2] = 7.17 µm.

Size (Lo) µm	Volume In %	Size (Hi) µm	Volume Below %
0.20	0.05	0.48	0.05
0.48	0.13	0.59	0.18
0.59	0.17	0.71	0.36
0.71	0.16	0.86	0.52
0.86	0.16	1.04	0.68
1.04	0.05	1.26	0.73
1.26	0.00	1.52	0.73
1.52	0.01	1.84	0.73
1.84	0.27	2.23	1.00
2.23	0.90	2.70	1.90
2.70	1.97	3.27	3.87
3.27	3.61	3.95	7.48
3.95	5.82	4.79	13.30
4.79	8.46	5.79	21.76
5.79	11.15	7.01	32.91
7.01	13.30	8.48	46.21

Size (Lo) µm	Volume In %	Size (Hi) µm	Volume Below %
8.48	14.17	10.27	60.38
10.27	13.24	12.43	73.62
12.43	10.70	15.05	84.31
15.05	7.34	18.21	91.65
18.21	4.15	22.04	95.80
22.04	1.92	26.68	97.72
26.68	0.84	32.29	98.55
32.29	0.53	39.08	99.08
39.08	0.44	47.30	99.52
47.30	0.31	57.25	99.83
57.25	0.10	69.30	99.93
69.30	0.00	83.87	99.93
83.87	0.00	101.52	99.93
101.52	0.00	122.87	99.93
122.87	0.01	148.72	99.94
148.72	0.06	180.00	100.00

Malvern Instruments Ltd.
Malvern, U.K.

MasterSizer X Ver. 1.2b
Serial No.

29 Dec 95 09:49

Table A.3. Size distribution of 31.4 micron AP particles



**TÜRKİYE BİLİMSEL VE TEKNİK ARAŞTIRMA KURUMU
SAYUNMA SANAYİ ARAŞTIRMA VE GELİŞTİRME ENSTİTÜSÜ**

31 micron AP Run No. 1

Presentation: 2RHA
 Polydisperse model
 Sample: CEV-PSD, 20 Source: Averaged Volume Result
 Focus = 100 mm. Beam Length = 2.4 mm. Obscuration = 16.5 %

Measured on: 21 Apr 1995 09:54 Sampler: MSX64
 Analysed on: 21 Apr 1995 09:56
 Last Saved: 21 Apr 1995 09:57
 Configuration file: SIZER
 Sample Path: C:\SIZER\DATA\

Residual = 0.418 % Concentration = 0.021 %
 Uniformity = 0.843 Span = 2.622
 Specific S.A. = 0.3252 sq. m. /gm.
 d (v, 0.5) = 23.65 um Mode = 36.58 um D [4, 3] = 31.43 um
 d (v, 0.1) = 5.15 um d (v, 0.9) = 67.16 um D [3, 2] = 9.46 um.

Size (Lo) um	Volume In %	Size (Hi) um	Volume Below %
0.20	0.16	0.48	0.16
0.48	0.41	0.59	0.57
0.59	0.54	0.71	1.11
0.71	0.51	0.86	1.62
0.86	0.38	1.04	2.00
1.04	0.27	1.26	2.27
1.26	0.24	1.52	2.51
1.52	0.34	1.84	2.84
1.84	0.55	2.23	3.39
2.23	0.86	2.70	4.25
2.70	1.22	3.27	5.46
3.27	1.61	3.95	7.08
3.95	2.03	4.79	9.11
4.79	2.50	5.79	11.61
5.79	3.05	7.01	14.65
7.01	3.71	8.48	18.36

Size (Lo) um	Volume In %	Size (Hi) um	Volume Below %
8.48	4.47	10.27	22.83
10.27	5.24	12.43	28.08
12.43	5.93	15.05	34.00
15.05	6.47	18.21	40.47
18.21	6.89	22.04	47.36
22.04	7.28	26.68	54.64
26.68	7.71	32.29	62.36
32.29	8.02	39.08	70.38
39.08	7.81	47.30	78.18
47.30	6.98	57.25	85.17
57.25	5.66	69.30	90.83
69.30	4.02	83.87	94.84
83.87	2.43	101.52	97.27
101.52	1.29	122.87	98.57
122.87	0.78	148.72	99.34
148.72	0.66	180.00	100.00

Malvern Instruments Ltd.
Malvern, U.K.

MasterSizer X Ver. 1.2b
Serial No.

29 Dec 95 09:52

Table A.4. Size distribution of 171 micron AP particles



**TÜRKİYE BİLİMSEL VE TEKNİK ARAŞTIRMA KURUMU
SAYUNMA SANAYİ ARAŞTIRMA VE GELİŞTİRME ENSTİTÜSÜ**

171 micron AP		Run No. 1
Presentation: 2RHA		Volume Result
Polydisperse model		
Sample: CEV-PSD, 2	Source: Analysed	
Focus = 300 mm.	Beam Length = 2.4 mm.	Obscuration = 13.3 %

--

Measured on: 15 Nov 1994 12:24	Sampler: MSX64
Analysed on: 15 Nov 1994 13:24	
Last Saved: 15 Nov 1994 13:24	
Configuration file: SIZER	
Sample Path: C:\SIZER\DATA\	

Residual = 0.503 %	Concentration = 0.107 %	
Uniformity = 0.506	Span = 1.691	
Specific S.A. = 0.0523 sq. m. /gm.		
d (v, 0.5) = 160.36 um	Mode = 188.09 um	D [4, 3] = 171.12 um
d (v, 0.1) = 40.69 um	d (v, 0.9) = 311.89 um	D [3, 2] = 58.82 um.

Size (Lo) um	Volume In %	Size (Hi) um	Volume Below %
0.50	0.05	1.32	0.05
1.32	0.13	1.60	0.18
1.60	0.17	1.95	0.35
1.95	0.19	2.38	0.54
2.38	0.19	2.90	0.73
2.90	0.18	3.53	0.91
3.53	0.19	4.30	1.10
4.30	0.23	5.24	1.33
5.24	0.29	6.39	1.62
6.39	0.36	7.78	1.98
7.78	0.43	9.48	2.41
9.48	0.51	11.55	2.91
11.55	0.58	14.08	3.50
14.08	0.70	17.15	4.19
17.15	0.86	20.90	5.05
20.90	1.10	25.46	6.16

Size (Lo) um	Volume In %	Size (Hi) um	Volume Below %
25.46	1.41	31.01	7.56
31.01	1.72	37.79	9.28
37.79	2.01	46.03	11.29
46.03	2.35	56.09	13.64
56.09	2.96	68.33	16.60
68.33	4.09	83.26	20.69
83.26	5.91	101.44	26.60
101.44	8.35	123.59	34.95
123.59	11.02	150.57	45.97
150.57	13.09	183.44	59.07
183.44	13.35	223.51	72.42
223.51	11.49	272.31	83.91
272.31	8.36	331.77	92.26
331.77	5.23	404.21	97.49
404.21	2.51	492.47	100.00
492.47	0.00	600.00	100.00

Malvern Instruments Ltd.
Malvern, U.K.

MasterSizer X Ver. 1.2b
Serial No.

29 Dec 95 09:55

Table A.5. Size distribution of 323 micron AP particles



**TÜRKİYE BİLİMSEL VE TEKNİK ARAŞTIRMA KURUMU
SAVUNMA SANAYİİ ARAŞTIRMA VE GELİŞTİRME ENSTİTÜSÜ**

323 micron AP		Run No. 1
Presentation: 2RHA		Volume Result
Polydisperse model		
Sample: AP 121	Source: Averaged	
Focus = 300 mm.	Beam Length = 2.4 mm.	Obscuration = 14.3 %

--

Measured on: 15 Nov 1994 11:55	Sampler: MSX64
Analysed on: 15 Nov 1994 12:02	
Last Saved: 15 Nov 1994 12:06	
Configuration file: SIZER	
Sample Path: C:\SIZER\DATA\	

Residual = 0.936 %	Concentration = 0.185 %	
Uniformity = 0.401	Span = 1.333	
Specific S.A. = 0.0266 sq. m. /gm.		
d (v, 0.5) = 329.95 um	Mode = 0.00 um	D [4, 3] = 323.46 um
d (v, 0.1) = 98.05 um	d (v, 0.9) = 537.73 um	D [3, 2] = 115.71 um.

Size (Lo) um	Volume In %	Size (Hi) um	Volume Below %
0.50	0.04	1.32	0.04
1.32	0.08	1.60	0.12
1.60	0.07	1.95	0.20
1.95	0.08	2.38	0.27
2.38	0.07	2.90	0.34
2.90	0.07	3.53	0.41
3.53	0.07	4.30	0.48
4.30	0.08	5.24	0.56
5.24	0.11	6.39	0.66
6.39	0.14	7.78	0.81
7.78	0.18	9.48	0.99
9.48	0.22	11.55	1.21
11.55	0.25	14.08	1.46
14.08	0.29	17.15	1.75
17.15	0.34	20.90	2.09
20.90	0.41	25.46	2.50

Size (Lo) um	Volume In %	Size (Hi) um	Volume Below %
25.46	0.51	31.01	3.01
31.01	0.66	37.79	3.66
37.79	0.84	46.03	4.50
46.03	1.06	56.09	5.56
56.09	1.30	68.33	6.86
68.33	1.57	83.26	8.44
83.26	1.92	101.44	10.36
101.44	2.46	123.59	12.83
123.59	3.38	150.57	16.20
150.57	4.87	183.44	21.07
183.44	6.99	223.51	28.06
223.51	9.70	272.31	37.76
272.31	12.62	331.77	50.38
331.77	15.14	404.21	65.52
404.21	16.63	492.47	82.15
492.47	17.85	600.00	100.00

Malvern Instruments Ltd.
Malvern, U.K.

MasterSizer X Ver. 1.2b
Serial No.

29 Dec 95 09:57

APPENDIX B

MODEL AND OPTIMUM SIZE DISTRIBUTIONS

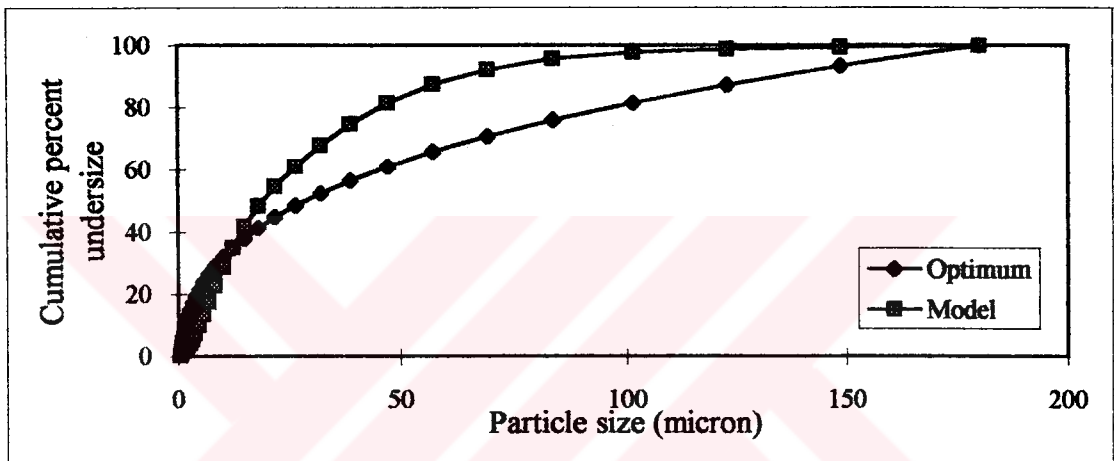


Figure B.1. Comparison of model and optimum distributions for Set No 1

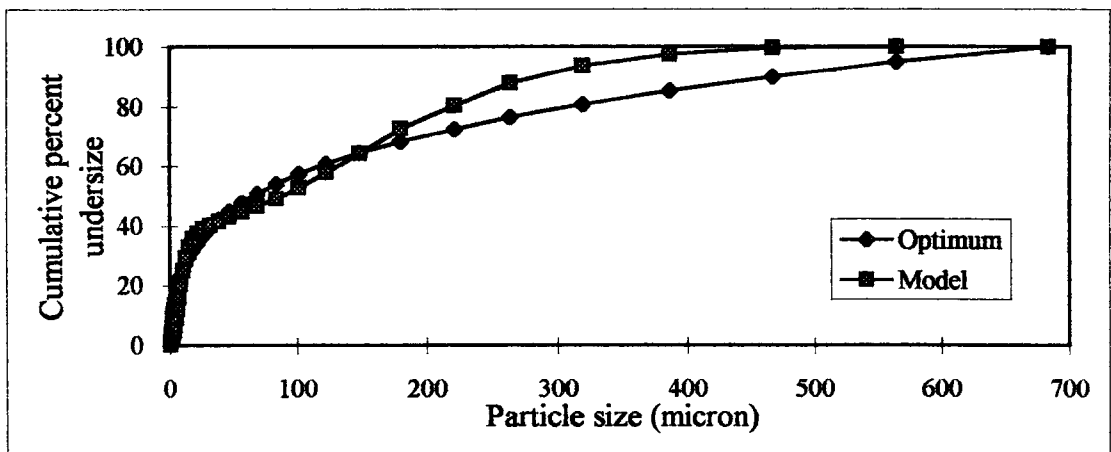


Figure B.2. Comparison of model and optimum distributions for Set No 2

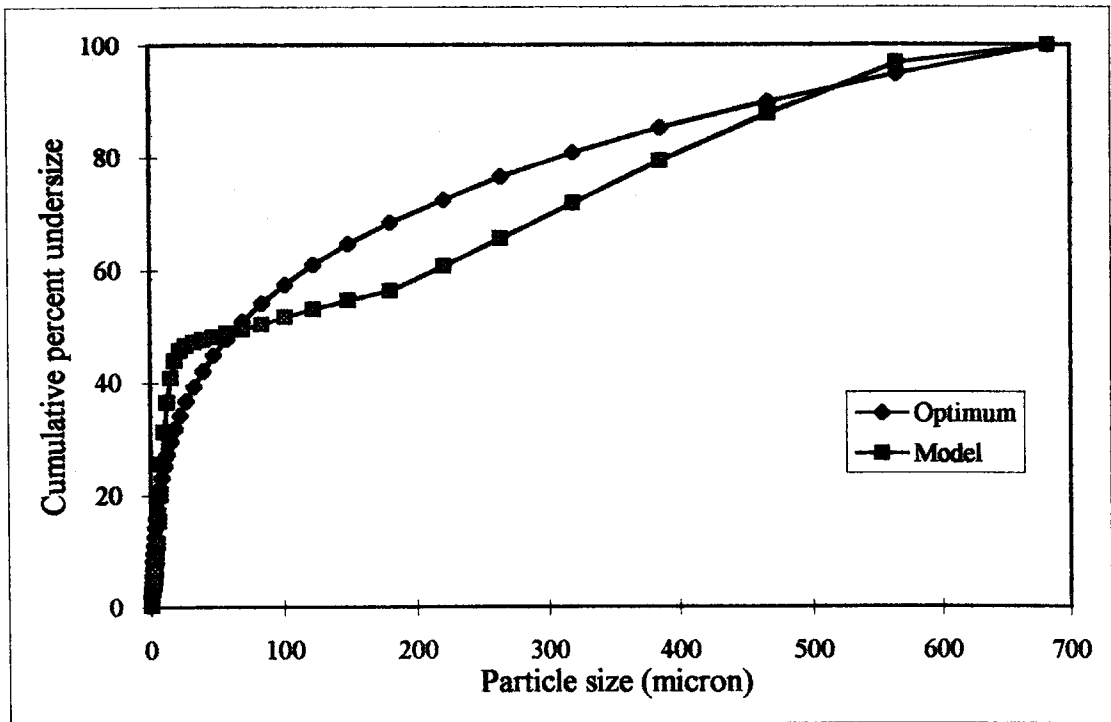


Figure B.3. Comparison of model and optimum distributions for Set No 3

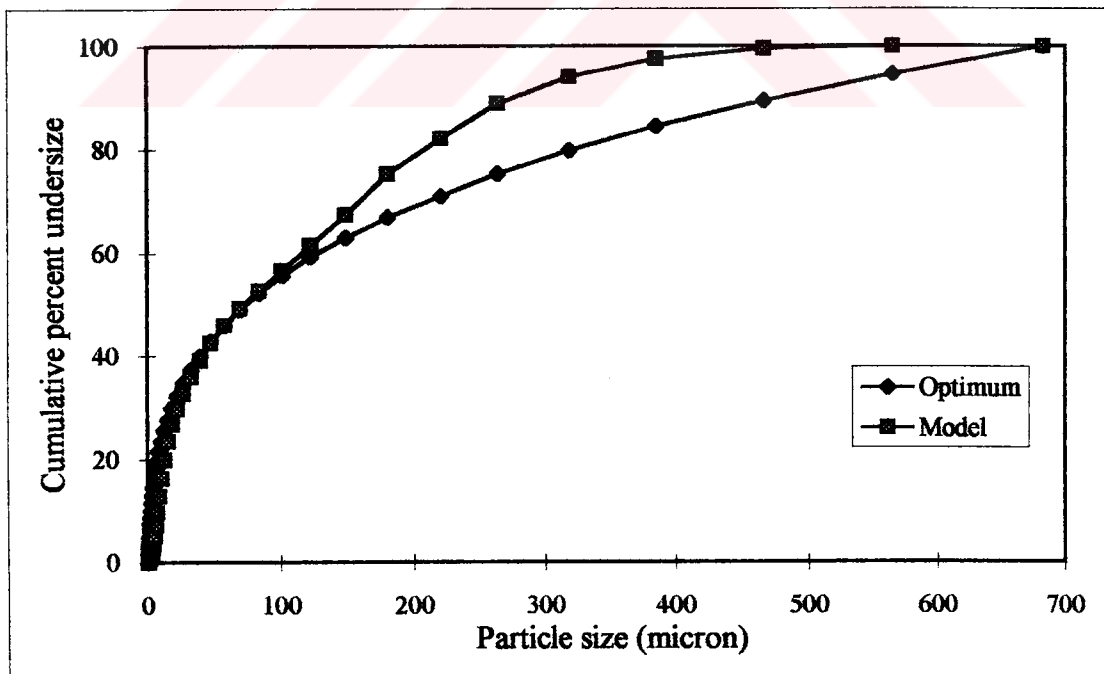


Figure B.4. Comparison of model and optimum distributions for Set No 4

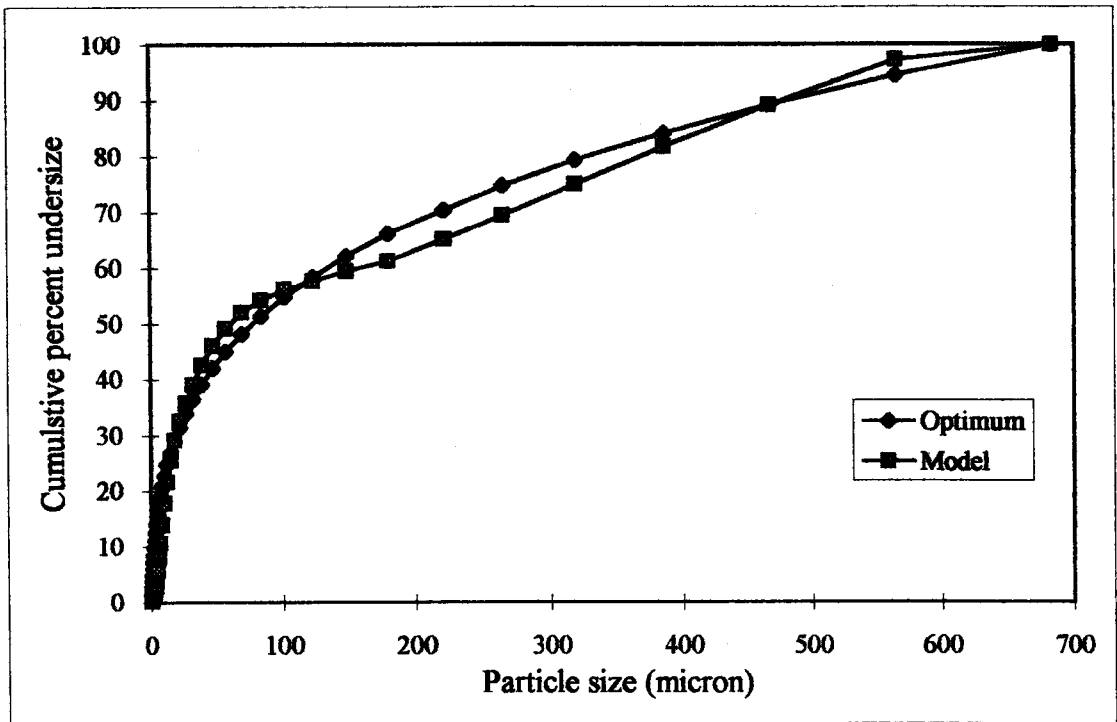


Figure B.5. Comparison of model and optimum distributions for Set No 5

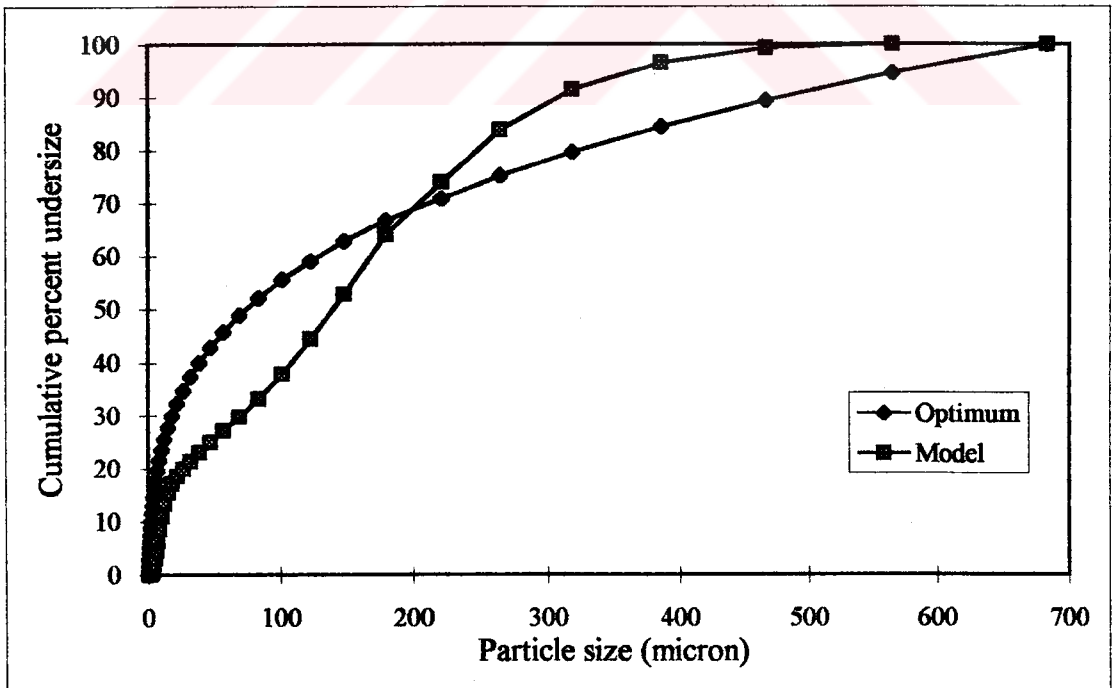


Figure B.6. Comparison of model and optimum distributions for Set No 6

APPENDIX C

Table C.1. Results of viscosity measurements at different shear rates

Time (sec)	Rate of shear (RPM)						Rate of shear (RPM)				
	0.5	1	2.5	5	10		0.5	1	2.5	5	10
	Viscosity, Poise						Viscosity, Poise				
0	3580	2430	1940	1700	1550		736	832	792	784	790
10	3680	2350	1910	1680	1510		768	832	788	780	787
20	3800	2370	1910	1660	1500		800	832	788	774	786
24					1500						784
30	3640	2400	1910	1660			800	816	780	774	781
40	3360	2340	1870	1650			800	816	780	772	
48				1650						768	
50	3420	2350	1880				832	816	780		
60	3420	2320	1850				832	816	776		
70	3460	2270	1850				832	816	776		
80	3480	2270	1830				832	816	776		
90	3480	2300	1820				864	832	776		
96			1820						776		
100	3300	2270					832	800			
110	3200	2270					864	816			
120	3200	2270					864	816			
130	3240	2220					864	800			
140	3240	2220					864	816			
150	3260	2260					864	816			
160	3240	2220					864	800			
170	3100	2210					864	800			
180	3040	2180					864	800			
190	3040	2180					864	800			
200	3080	2140					864	816			
210	3100	2180					864	800			
220	3140	2180					864	800			
230	3000	2160					864	800			
240	2880	2140					864	800			
250	2880						864				
260	2920						864				
270	2940						864				
280	2940						864				
290	2940						864				
300	2880						864				
310	2820						864				
320	2840						864				
330	2840						864				
340	2840						864				
350	2820						864				
360	2820						864				
370	2760						864				
380	2680						864				
390	2720						864				
400	2760						864				
410	2720						864				
420	2720						864				
430	2660						864				
440	2680						864				
450	2680						864				
460	2680						864				
470	2680						864				
480	2680						864				

(a) No Z, $F_{mes}=0.1$

(b) No Z, $F_{mes}=0.24$

Table C. 1(Continued) Results of viscosity measurements

Time (sec)	Rate of shear (RPM)						Rate of shear (RPM)				
	0.5	1	2.5	5	10		0.5	1	2.5	5	10
	Viscosity, Poise						Viscosity, Poise				
0	1180	1280	1260	1300	1420		1410	1120	884	772	682
10	1220	1280	1250	1290	1410		1540	1100	884	748	685
20	1220	1260	1240	1290	1410		1790	1120	852	730	678
24					1410						685
30	1220	1260	1240	1290			1920	1100	876	730	
40	1250	1260	1240	1290			1820	1100	852	724	
48				1290						720	
50	1250	1260	1230				1630	1120	824		
60	1250	1260	1230				1440	1090	840		
70	1250	1260	1220				1410	1070	844		
80	1280	1260	1230				1570	1100	832		
90	1280	1260	1230				1730	1060	808		
96			1230						824		
100	1310	1260					1730	1100			
110	1310	1250					1540	1070			
120	1310	1260					1440	1040			
130	1310	1260					1380	1040			
140	1310	1260					1380	1060			
150	1340	1260					1540	1040			
160	1340	1260					1540	1020			
170	1340	1260					1470	1040			
180	1340	1260					1440	1020			
190	1340	1260					1340	976			
200	1340	1260					1310	1010			
210	1340	1250					1470	992			
220	1340	1250					1470	992			
230	1340	1260					1440	1010			
240	1340	1260					1380	1010			
250	1380						1380				
260	1380						1340				
270	1340						1380				
280	1340						1410				
290	1340						1380				
300	1380						1380				
310	1380						1310				
320	1380						1250				
330	1380						1380				
340	1380						1310				
350	1340						1340				
360	1340						1380				
370	1340						1340				
380	1380						1280				
390	1380						1280				
400	1340						1340				
410	1380						1280				
420	1380						1280				
430	1380						1280				
440	1380						1280				
450	1380						1280				
460	1380						1250				
470	1380						1280				
480	1380						1250				

(c) No 2, Fines=0.4

(d) No 3, Fines=0.04

Table C.1(Continued). Results of viscosity measurements

Time (sec)	Rate of shear (RPM)						Rate of shear (RPM)				
	0.5	1	2.5	5	10		0.5	1	2.5	5	10
	Viscosity, Poise						Viscosity, Poise				
0	672	672	608	566	541		672	672	652	668	707
10	640	672	596	556	526		640	672	660	668	707
20	704	656	588	548	528		672	672	660	668	701
24					523						694
30	704	656	584	548			672	672	652	668	
40	672	656	588	540			704	656	652	668	
48				540						668	
50	704	640	576				704	672	652		
60	704	640	576				672	656	648		
70	672	640	576				672	672	648		
80	672	624	568				672	656	648		
90	672	640	568				704	672	648		
96			564						648		
100	704	640					704	672			
110	704	640					704	656			
120	704	640					704	656			
130	704	640					704	672			
140	672	640					704	672			
150	672	640					672	656			
160	672	640					672	656			
170	704	640					704	656			
180	704	624					704	656			
190	704	624					704	656			
200	704	640					672	656			
210	704	640					704	672			
220	704	640					704	656			
230	704	640					704	656			
240	704	640					704	656			
250	704						704				
260	704						704				
270	704						704				
280	704						704				
290	704						704				
300	704						704				
310	704						704				
320	704						704				
330	704						704				
340	704						704				
350	704						704				
360	704						704				
370	704						704				
380	704						704				
390	704						704				
400	704						704				
410	704						704				
420	704						704				
430	736						704				
440	736						704				
450	704						704				
460	704						704				
470	704						704				
480	704						704				

(e) No 3, Fines=0.15

(f) No 3, Fines=0.3272

Table C.1(Continued). Results of viscosity measurements

Time (sec)	Rate of shear (RPM)						Rate of shear (RPM)				
	0.5	1	2.5	5	10		0.5	1	2.5	5	10
	Viscosity, Poise						Viscosity, Poise				
0	1150	1360	1380	1430	1550		3680	2500	2040	1340	856
10	1180	1360	1360	1430	1550		3800	2620	1810	1200	840
20	1250	1380	1350	1420	1550		3800	2800	1820	1190	832
24					1540						832
30	1250	1380	1370	1410			3680	2380	1890	1160	
40	1280	1360	1360	1410			3740	2720	1840	1160	
48				1430						1160	
50	1280	1360	1350				3620	2720	1790		
60	1310	1360	1360				3680	2670	1770		
70	1310	1380	1360				3740	2780	1760		
80	1310	1340	1360				3620	2700	1760		
90	1310	1340	1360				3620	2770	1760		
96			1350						1740		
100	1340	1340					3640	2670			
110	1380	1360					3460	2690			
120	1340	1360					3720	2780			
130	1380	1380					3720	2590			
140	1380	1380					3640	2620			
150	1380	1390					3740	2660			
160	1380	1360					3720	2560			
170	1380	1390					3800	2560			
180	1410	1380					3720	2610			
190	1410	1380					3520	2700			
200	1410	1380					3620	2590			
210	1410	1380					3460	2590			
220	1410	1380					3620	2580			
230	1410	1380					3800	2580			
240	1410	1380					3640	2590			
250	1440						3560				
260	1410						3480				
270	1410						3560				
280	1440						3680				
290	1470						3580				
300	1440						3640				
310	1440						3780				
320	1410						3480				
330	1440						3560				
340	1470						3320				
350	1440						3260				
360	1440						3620				
370	1440						3480				
380	1440						3360				
390	1440						3520				
400	1440						3400				
410	1470						3460				
420	1470						3720				
430	1470						3400				
440	1470						3400				
450	1470						3460				
460	1500						3240				
470	1470						3580				
480	1470						3520				

(g) No 3, Fines=0.5

(h) No 4, Fines=0.1

Table C.1(Continued). Results of viscosity measurements

Time (sec)	Rate of shear (RPM)						Rate of shear (RPM)				
	0.5	1	2.5	5	10		0.5	1	2.5	5	10
	Viscosity, Poise						Viscosity, Poise				
0	1060	1120	1030	980	944		896	1010	984	964	952
10	1090	1120	1030	976	936		928	992	968	960	952
20	1090	1120	1030	966	928		960	992	972	956	944
24					928						936
30	1120	1120	1020	970			992	992	968	950	
40	1150	1100	1020	966			992	992	968	950	
48				966						950	
50	1120	1100	1020				992	992	972		
60	1150	1090	1010				992	992	960		
70	1180	1100	1020				992	992	960		
80	1180	1100	1010				992	992	952		
90	1180	1120	1000				1020	992	960		
96			1000						960		
100	1150	1090					1020	992			
110	1180	1100					1020	992			
120	1180	1090					1020	992			
130	1180	1090					1020	992			
140	1180	1090					1020	992			
150	1180	1090					1020	992			
160	1180	1090					1020	992			
170	1180	1090					1020	1010			
180	1180	1070					1020	992			
190	1180	1090					1020	992			
200	1180	1090					1020	992			
210	1180	1090					1020	992			
220	1220	1090					1020	992			
230	1220	1090					1020	992			
240	1220	1090					1020	992			
250	1150						1060				
260	1180						1020				
270	1180						1020				
280	1180						1020				
290	1180						1020				
300	1220						1060				
310	1220						1020				
320	1180						1060				
330	1180						1020				
340	1220						1060				
350	1220						1020				
360	1180						1020				
370	1180						1020				
380	1180						1020				
390	1180						1060				
400	1180						1020				
410	1180						1060				
420	1180						1060				
430	1180						1060				
440	1180						1060				
450	1180						1020				
460	1180						1020				
470	1180						1020				
480	1180						1060				

(i) No 4, Fines=0.27

(j) No 4, Fines=0.4

Table C.1(Continued). Results of viscosity measurements

Time (sec)	Rate of shear (RPM)						Rate of shear (RPM)				
	0.5	1	2.5	5	10		0.5	1	2.5	5	10
	Viscosity, Poise						Viscosity, Poise				
0	992	1170	1170	1180	1180		576	560	500	468	438
10	1060	1170	1160	1170	1180		608	560	488	460	432
20	1090	1170	1170	1170	1170		608	560	488	454	434
24					1170						429
30	1090	1170	1160	1160			640	560	488	452	
40	1120	1170	1160	1160			640	544	488	454	
48				1160						448	
50	1120	1170	1160				608	544	480		
60	1120	1170	1150				640	544	488		
70	1150	1150	1160				608	544	472		
80	1150	1170	1150				640	544	480		
90	1150	1170	1150				608	544	472		
96			1150						472		
100	1150	1170					640	544			
110	1180	1170					640	528			
120	1150	1150					640	528			
130	1150	1150					640	544			
140	1180	1170					608	528			
150	1180	1170					608	528			
160	1180	1170					640	512			
170	1180	1150					640	528			
180	1180	1170					640	528			
190	1180	1150					640	528			
200	1180	1170					640	512			
210	1180	1170					608	528			
220	1180	1170					608	528			
230	1180	1170					640	528			
240	1180	1170					608	512			
250	1180						608				
260	1220						608				
270	1220						608				
280	1180						640				
290	1180						608				
300	1220						640				
310	1220						640				
320	1180						608				
330	1220						608				
340	1220						608				
350	1220						608				
360	1220						608				
370	1220						608				
380	1220						608				
390	1220						608				
400	1220						608				
410	1220						608				
420	1220						640				
430	1220						640				
440	1220						608				
450	1220						608				
460	1220						576				
470	1220						608				
480	1220						608				

(k) No 4, Fines=0.52

(l) No 5, Fines=0.15

Table C.1(Continued). Results of viscosity measurements

Time (sec)	Rate of shear (RPM)						Rate of shear (RPM)				
	0.5	1	2.5	5	10		0.5	1	2.5	5	10
	Viscosity, Poise						Viscosity, Poise				
0	512	496	468	452	446		512	528	512	508	512
10	512	496	460	448	445		544	512	504	508	506
20	512	496	460	448	442		544	528	512	508	509
24					438						507
30	512	496	460	448			544	528	512	502	
40	544	496	456	444			544	528	504	502	
48				442						506	
50	544	496	456				544	528	504		
60	544	480	460				544	528	512		
70	544	480	448				544	512	500		
80	544	480	448				544	528	504		
90	544	490	448				512	512	504		
96			456						504		
100	544	490					544	528			
110	544	480					544	528			
120	544	496					544	528			
130	544	480					544	512			
140	544	480					544	512			
150	544	496					544	512			
160	544	496					544	528			
170	544	480					544	528			
180	544	496					544	528			
190	544	480					544	512			
200	544	480					544	512			
210	544	480					544	528			
220	544	480					544	528			
230	512	480					544	528			
240	512	480					544	512			
250	544						544				
260	544						544				
270	544						544				
280	544						544				
290	544						544				
300	512						544				
310	544						544				
320	544						544				
330	544						544				
340	544						544				
350	544						544				
360	544						544				
370	544						544				
380	544						544				
390	512						544				
400	544						544				
410	544						544				
420	544						544				
430	544						544				
440	544						544				
450	544						544				
460	544						544				
470	544						544				
480	544						544				

(m) No 5, Fines=0.3

(n) No 5, Fines=0.397

Table C.1(Continued). Results of viscosity measurements

Time (sec)	Rate of shear (RPM)					0.5	Rate of shear (RPM)			
	0.5	1	2.5	5	10		1	2.5	5	10
	Viscosity, Poise						Viscosity, Poise			
0	736	816	824	844	864		960	640	576	512
10	736	816	824	848	856		960	640	576	544
20	768	816	824	844	856		960	640	576	544
24					848					544
30	800	816	824	836			960	640	576	
40	800	816	820	836			960	640	576	
48				832					576	
50	800	816	820				960	640		
60	800	800	824				640	640		
70	800	800	820				960	640		
80	800	816	812				960	640		
90	800	800	820				960	640		
96			824				960	640		
100	832	800					960			
110	832	800					960			
120	800	816					640			
130	800	800					960			
140	832	816					960			
150	832	816					960			
160	800	816					960			
170	832	800					960			
180	832	800					640			
190	832	816					960			
200	800	816					960			
210	832	816					960			
220	832	816					960			
230	832	816					960			
240	800	800					960			
250	832									
260	832									
270	832									
280	832									
290	832									
300	832									
310	832									
320	832									
330	832									
340	832									
350	832									
360	832									
370	832									
380	832									
390	832									
400	832									
410	832									
420	832									
430	832									
440	832									
450	832									
460	832									
470	832									
480	832									

(o) No 5, Fines=0.55

(p) Unfilled polymer matrix

F. O. YOUNG ET AL. IN PROCEEDINGS OF THE 1984 CONFERENCE ON POLYMERIZATION AND RHEOLOGY